Targeting selectively oxytocin receptor signalling efficiently improves social interaction in Fmr1 KO mice

Caroline Gora, Nicolas Azzopardi, Lucile Drobecq, Emmanuel Pecnard, Patrick Schnider, Pascale David-Pierson, Romain Yvinec, Christophe Grundschober, Lucie P. Pellissier

Title: **Targeting selectively oxytocin receptor signalling efficiently improves social interaction in *Fmr1* KO mice**

Running title: **Selective OTR agonists restore sociability in *Fmr1* KO mice**

Caroline GORA[1#*], Nicolas AZZOPARDI[1#], Lucile DROBECQ[1], Emmanuel PECNARD[1], Patrick SCHNIDER[2], Pascale DAVID-PIERSON[3], Romain YVINEC[1,4], Christophe GRUNDSCHOBER[5], and Lucie P. PELLISSIER[1*]

[1]INRAE, CNRS, Université de Tours, PRC, 37380, Nouzilly, France

[2]Roche Pharma Research and Early Development, Therapeutic Modalities, Roche Innovation Center Basel, F. Hoffmann-La Roche AG, Basel, Switzerland

[3]Roche Pharma Research and Early Development, Pharmaceutical Science, Roche Innovation Center Basel, F. Hoffmann-La Roche AG, Basel, Switzerland

[4]Université Paris-Saclay, Inria, Centre Inria de Saclay, 91120, Palaiseau, France

[5]Roche Pharma Research and Early Development, Neuroscience Discovery, Roche Innovation Center Basel, F. Hoffmann-La Roche AG, Basel, Switzerland

[#]authors contributed equally

*corresponding authors: Caroline Gora and Lucie P. Pellissier, PhD, Team biology of GPCR Signalling systems (BIOS), INRAE, CNRS, Université de Tours, PRC, 37380, Nouzilly, France. Phone: +33 4 47 42 79 62. Emails: caroline.gora@inrae.fr and lucie.pellissier@inrae.fr

Word count: 3570/4000 (excluding abstract, methods, references and figure legends)

ACKNOWLEDGEMENTS

Mouse breeding and care was performed at INRAE Animal Physiology Facility (https://doi.org/10.15454/1.5573896321728955E12). This project has received funding from the European Research Council (ERC) under the European Union's Horizon 2020 research and innovation programme (grant agreement No. 851231). We thank Dr Pascale Crépieux and Dr Eric Reiter for their advice on the manuscript. LPP and CG acknowledge the LabEx MabImprove (grant ANR-10-LABX-53-01) for the financial support in co-financing CG's PhD fellowship. We used ChatGPT, developed by OpenAI, for assistance with English editing. The conducted research was not preregistered with an analysis plan in an independent, institutional registry.

CONFLICT OF INTEREST STATEMENT

PDP, PS and ChG are or were employed by F. Hoffmann-La Roche AG, Basel, Switzerland.

The other authors declare no conflict of interest.

BULLET POINT SUMMARY

What is already known

- Drugs, including OT and AVP, are inefficient to improve social impairments in individuals with autism
- Targeting OTR and V_{1A} receptors remains the most relevant option for the management of autism.

What does this study add

- Selective OTR agonists biased towards Gαq signalling improve sociability in *Fmr1* KO mice.
- The V_{1A} antagonist RO6893074 is not sufficient to improve sociability in *Fmr1* KO mice.

What is the clinical significance

- Selective Gαq-biased OTR agonists represent a promising strategy for the management of autism.

ABSTRACT

Background and Purpose: No drugs targeting the core social features of autism spectrum disorder (ASD) have been approved. Although clinical trials with oxytocin (OT) and vasopressin (AVP) have yielded mixed results, targeting their receptors remains the most promising pharmacological strategy for addressing social impairments in ASD. This study aims to identify which receptors and signalling pathways within this family can sustainably improve social impairments.

Experimental Approach: We used dose-response and kinetic analyses, along with mathematical modelling, to evaluate OT, AVP, their homologs, and novel synthetic ligands on G protein coupling, β-arrestins recruitment, and internalisation of mouse oxytocin (OTR) and vasopressin (V_{1A}, V_{1B}, V_2) receptors in Neuro-2a cells. We tested acute and subchronic administration of OTR agonists and the novel V_{1A} receptor antagonist, alongside OT and AVP, for their effects on social interaction in *Fmr1* KO mice, a model exhibiting ASD-like features.

Key Results: While OT, AVP and most compounds were non-selective across the four receptors, the OTR agonists TGOT or RO6958375 and the V_{1A} antagonist RO6893074 were selective. TGOT or RO6958375, favouring $G\alpha_q$ signalling, enhanced social interactions in *Fmr1* KO mice while showing minimal effects in wild-type mice. In contrast, OT, AVP or RO6893074 exhibited limited efficacy in *Fmr1* KO mice.

Conclusion and Implications: Selective OTR agonists, unlike OT and AVP, effectively improved social impairments in *Fmr1* KO mice after acute and subchronic treatment. These findings

highlight the necessity for developing highly selective OTR $G\alpha_q$-biased agonists to achieve clinical outcomes in ASD.

Keywords (3-7 words): **oxytocin receptors, vasopressin receptors, G protein-coupled receptors, signalling pathways, autism spectrum disorder, Fragile X syndrome, social interaction**

INTRODUCTION

Autism spectrum disorder (ASD) is a neurodevelopmental condition characterised by impairments in social communication and interaction, along with stereotyped or repetitive behaviours (American Psychiatric Association, 2013). It affects approximately 1% of the global population (Zeidan et al., 2022). Recent genome-wide association studies have identified hundreds of candidate genes (SFARI Gene), implicating convergent neurobiological mechanisms such as gene expression regulation and neuronal communication, signalling or plasticity (De Rubeis et al., 2014; Satterstrom et al., 2020; Pintacuda et al., 2023). Fragile X syndrome, a monogenic disorder frequently associated with ASD and intellectual disability, results from the loss of FMRP expression (Pieretti et al., 1991; Verheij et al., 1993). To date, no effective pharmacological options targeting core social features have been approved for individuals with ASD. Placebo effects, lack of efficacy, and the heterogeneity of patients within the spectrum have prevented success in phase 3 clinical trials.

G protein-coupled receptors (GPCRs), are targeted by around 30% of approved drugs (Hauser et al., 2017; Alexander et al., 2021) and are key regulators of downstream signalling that are dysregulated in ASD (De Rubeis et al., 2014; Satterstrom et al., 2020; Pintacuda et al., 2023). Over 200 pathogenic variants in 26 GPCR genes have been associated with ASD (SFARI Gene, Annamneedi et al., 2023). Thus, GPCRs have emerged as robust and specific therapeutic targets for ASD. Among them, oxytocin (OT) or vasopressin (AVP) bind to oxytocin (OTR) and vasopressin (V_{1A} and V_{1B}) receptors in the brain, modulating social behaviours (Busnelli et al., 2013; Quintana et al., 2019; Rigney et al., 2022; Theofanopoulou et al., 2022). These receptors are primarily coupled to $G\alpha_{q/11}$ proteins, leading to the activation of the IP_3-Ca^{2+} signalling pathway and recruit β-arrestins upon ligand binding (Busnelli et al., 2013). Although results have been inconsistent, some clinical trials have reported improvements in social scales and

repetitive behaviours following intranasal administration of OT (Bernaerts et al., 2020; Annamneedi et al., 2023; Daniels et al., 2023; Guastella et al., 2023). Notably, while plasma and brain concentrations of OT are not correlated (Valstad et al., 2017; Gora et al., 2024), individuals with lower plasma OT levels tend to respond better to exogenous OT administration (Parker et al., 2017). Furthermore, recent studies suggest that combining OT administration with behavioural interventions enhances sociability more than OT alone (Ford and Young, 2022; Daniels et al., 2023; Pantouli et al., 2024). Similarly intranasal AVP administration was well tolerated in early trials and improved social responsiveness, particularly in children with ASD and low plasma AVP concentrations (Parker et al., 2019). While administration of the V_{1A} antagonists balovaptan or RG7713 enhanced social skills in adults with ASD in phase 2 or exploratory clinical studies (Umbricht et al., 2017; Bolognani et al., 2019), balovaptan did not show improvement over placebo in phase 3 trials (Hollander et al., 2022; Jacob et al., 2022). Despite this, OTR and V_{1A} receptors remain the most promising targets to improve sociability in individuals with ASD (Annamneedi et al., 2023). Further research is needed to identify the most suitable ligands, targets and downstream signalling pathways.

In this study, we aim to enhance our understanding of why compounds targeting OTR and V_{1A} receptors have underperformed in clinical trials. We used a systematic pharmacological approach to assess both existing and novel ligands, determining which ligand-receptor pairings are most promising *in vitro* and in *Fragile X Mental Retardation 1* knockout (*Fmr1* KO) mice.

RESULTS

Oxytocin or vasopressin act as partial agonists on mouse vasopressin or oxytocin receptors in murine Neuro-2a cells

To address the inconsistent results from OT and AVP clinical trials, it is essential to investigate their distinct pharmacological profiles on OTR, V_{1A}, V_{1B} and V_2 receptors. We assessed their kinetics and concentration-response relationships across the four murine receptors, evaluating ten signalling outputs in the murine Neuro-2a neuroblastoma cell line, using BRET1 assays over a 30-min period and luminescence assay for Ca^{2+} release (Figure 1A). Spider plots illustrated that all receptors recruited miniGq, leading to intracellular Ca^{2+} mobilisation, and both β-arrestin-1 and -2 and internalised (using CAAX and FYVE sensors) following OT or AVP stimulation (Figures 1C, S1, Table S1). As expected, V_2 also recruited miniGs and induced cAMP production. None of the receptors recruited miniGi or reduced forskolin-induced cAMP production. Overall, AVP acted as a partial agonist on OTR compared to OT, while OT was a partial agonist on V_{1A} receptors across these assays (except for Ca^{2+} mobilisation). OT acted as a full agonist with lower potency than AVP on V_{1B} and V_2 receptors, although it was less efficient at recruiting β-arrestin on V_2 receptors (Figures 1C, S1). The pharmacological profiles of OT and AVP for the four human receptors in human HEK293A cells were comparable to those observed for the murine receptors (Figure S2, Table S2).

To estimate the potential role of receptor internalisation in the lack of efficacy resulting from repeated OT and AVP administration during clinical trials, we quantified the β-arrestin recruitment and receptor internalisation kinetics for the four receptors using mathematical modelling (Figure 1B). The model (**1**), which incorporates receptor internalisation, β-arrestin recruitment, and subsequent receptor recycling, provided the best fit for the BRET1 data (Material and Methods, Figure S3, Table S3). The parameter identifiability procedure yielded

151 robust normalised parameter estimation with small confidence intervals for predicted affinity
152 ($1/K_D$) and for kinetic parameters, β-arrestin recruitment (k_τ), internalisation (k_{int}) and
153 recycling (k_{rec}; Table S3), except for OT on the V_{1A} receptor and AVP on OTR where the E_{max}
154 were not reached. We found that receptor recycling was statistically significant except for
155 AVP on OTR, and was slower than internalisation within the 30-minute period ($k_{rec} \approx 0.1$ min^{-1}
156 and slightly higher for AVP on V_2 receptor; Figure 1D, Table S3). Radar plots highlighted key
157 differences in kinetic parameters, showing that OT on OTR, OT and AVP on V_{1B} and AVP on V_{1A}
158 and V_2 receptors shared similar parameter landscapes, and to a lesser extent, OT on V_2 (Figure
159 1D, Table S3). These ligand-receptor pairings exhibited comparatively higher affinity ($1/K_D$),
160 recycling (k_{rec}) and internalisation (k_{int}) rates, along with lower β-arrestin recruitment (k_τ).
161 Conversely, despite large confidence intervals, AVP on OTR and OT on V_{1A} receptors showed
162 lower affinity ($1/K_D$) and internalisation (k_{int}), and higher β-arrestin recruitment (k_τ, Table S3).
163 Using GPCR ligand bias analyses (Kolb et al., 2022), we found that AVP was significantly biased
164 towards miniGq on the OTR compared to OT (Figure 2A, Table 1). OT and AVP did not induce
165 any other significant biased signalling on the OTR, V_{1A} and V_{1B} receptors, as both G protein

and β-arrestin recruitment profiles were similar (Figure 2A). Overall, miniGq and β-arrestin-2 recruitment served as discriminant BRET1 assays to identify ligand bias (Table 1).

In conclusion, while OT and AVP activated all four receptors, with distinct potency and efficacy, they induced similar β-arrestin recruitment and receptor internalisation profiles. Only AVP displayed a partial biased agonist profile at the OTR.

Revisiting existing and novel ligands targeting oxytocin and vasopressin receptors in Neuro-2a cells

To identify the most specific and potentially biased ligands, we compared various agonists and antagonists targeting oxytocin and vasopressin receptors, focusing on miniGq and β-arrestin-2 recruitment in Neuro-2a cells (Figures 2, S4, Tables 1, S1).

The bird and fish OT homologues mesotocin and isotocin recruited both miniGq and β-arrestin-2 at all the four receptors, except for isotocin on the V_{1A} receptor (Figures 2A, S4A, Tables 1, S1). Notably, mesotocin and isotocin were biased towards miniGq on OTR, V_{1A} and V_2 receptors and on OTR, V_{1B} and V_2 receptors respectively, compared to OT and AVP. The bird AVP homologue vasotocin was more efficient than AVP on OTR, V_{1A} and V_{1B} and displayed also a significant bias only for OTR (Figures 2A, S4A, Tables 1, S1).

Among synthetic peptide OTR agonists, RO6958375 (Janz et al., 2023) and TGOT (Elands et al., 1988) activated OTR, and to a lesser extent V_2 for RO6958375, but neither activated V_{1A} and V_{1B}, in contrast to OT (Figures 2B-C, Table S1). Both synthetic ligands were identified as miniGq-biased agonists on OTR, and V_2 receptors for RO6958375, being less potent and efficient in β-arrestin-2 recruitment (Figure 2B-C, Tables 1, S1). However, kB7-OT (Koehbach et al., 2013) and carbetocin previously described as a $G\alpha_q$-biased OTR agonist (Passoni et al.,

2016), did not activate the receptors in our experiments, except for V_2 with carbetocin showing a miniGq-biased profile (Figures 2B, S4B, Table S1).

The OTR antagonists atosiban (Goodwin et al., 1994) and L-371,257 (Williams et al., 1995) displayed additional antagonistic effects on V_{1A} and V_2, respectively (Figures 2D). In contrast, the novel V_{1A} antagonist RO6893074, related to balovaptan (Schnider et al., 2020), displayed high selectivity and did not block OTR, V_{1B} and V_2 receptors (Figures 2D). Furthermore, RO6893074 did not inhibit a selection of 47 human receptors, channels, transporters and enzymes when tested at 3 µM (Table S4). Notably, none of the antagonists exhibited partial agonist effects or any bias on the four oxytocin or vasopressin receptors when tested alone (Figure S4C).

In conclusion, TGOT and RO6958375 are selective, partial miniGq-biased agonists for OTR while RO6893074 is a selective V_{1A} antagonist. Therefore, these ligands, alongside the reference peptides OT and AVP, are of interest for assessing their effects on social interaction outcomes.

Oxytocin or vasopressin administration did not enhance social interactions in *Fmr1* KO mice

To better understand the mixed outcomes of previous clinical trials, we compared the effects of acute (Day 0) and subchronic (Day 7) intranasal administration of OT and AVP at doses of 0, 20 and 40 µg.kg^{-1} in WT and *Fmr1* KO mice (Figures 3, S5-7, Table S5). The *Fmr1* KO mouse model is well-established for studying Fragile X syndrome and ASD (Kat et al., 2022), affecting oxytocin neurons (Lewis et al., 2020; Gora et al., 2024). Using the Live Mouse Tracker (de Chaumont et al., 2019), which automatically assesses multiple parameters of social interaction among two unfamiliar sex-, treatment- and genotype-matched mice, we

212 confirmed that *Fmr1* KO mice displayed consistent social interaction impairments compared
213 to WT mice, in both sexes (Figure S5).
214 Neither acute nor subchronic intranasal administration of OT, regardless of dose, improved
215 nose contacts and huddling behaviours — two parameters of social exploration, in *Fmr1* KO
216 mice (Figures 3, S6), while acute administration of OT at 40 µg.kg^{-1} reduced their time spent
217 in 'move in contact' (Figure S6A). In contrast, acute administration of OT at 20 µg.kg^{-1}
218 enhanced nose contacts and reduced the time spent 'stop isolated' in WT animals,
219 irrespective of treatment duration, while the highest dose reduced stretch-attend postures
220 (SAP) — an index of anxious-like behaviours (Figures 3, S6). Acute intranasal administration
221 of AVP decreased the time spent in nose contacts and huddling behaviours in *Fmr1* KO mice
222 at 40 µg.kg^{-1}, while subchronic intranasal administration of AVP at 20 µg.kg^{-1} increased these
223 social parameters in this group (Figures 3B, S6, Table S5).
224 In conclusion, neither OT nor AVP efficiently improved social impairments in *Fmr1* KO mice,
225 while AVP affected social interaction in WT mice.
226
227 **Targeting selectively oxytocin receptors improves social interactions in *Fmr1* KO mice**
228 To determine whether selective targeting of OTR signalling, in contrast to non-selective OT,
229 could effectively enhance social interactions in *Fmr1* KO mice, we administered selective OTR
230 peptide agonists TGOT (intranasally, at 0, 20 and 40 µg.kg^{-1}) and RO6958375 (subcutaneously,
231 at 0, 0.03, 0.06 and 0.12 mg.kg^{-1}) in both WT and *Fmr1* KO mice (Figures 4, S7, Table S5). Acute
232 intranasal administration of TGOT at 20 µg.kg^{-1} increased social exploration in *Fmr1* KO mice,
233 as evidenced by enhanced nose contacts and huddling behaviours. Subchronic administration
234 of TGOT at 40 µg.kg^{-1} also increased nose contacts but did not affect other parameters in
235 *Fmr1* KO mice (Figure 4). In contrast, both acute and subchronic administration of TGOT at

the highest dose (40 µg.kg^{-1}) reduced all social parameters in WT mice and increased the time spent isolated and in SAP (Figures 4, S7). Both acute or subchronic administration of the OTR agonist RO6958375 at low (0.03 mg.kg^{-1}) and moderate (0.06 mg.kg^{-1}) doses increased social interaction in *Fmr1* KO mice, as well as social motivation ('social approach' and 'move in contact') at the moderate dose (Figures 4). Acute administration of the moderate dose also increased nose contacts and huddling behaviours in WT mice. However, subchronic exposure to the highest dose (0.12 mg.kg^{-1}) reduced social motivation and increased anxious-like behaviours in WT mice (Figures 4, S7).

We also tested the small compound V_{1A} antagonist RO6893074 (intraperitoneally at 0, 25, 50 and 100 mg.kg^{-1}) in both WT and *Fmr1* KO mice, aiming to redirect endogenous oxytocin release on OTR by blocking V_{1A} receptors (Figures 4, S7, Table S5). Acute administration of RO6893074 at 50 mg.kg^{-1} increased social interaction in *Fmr1* KO mice (Figure 4). However, administration at 100 mg.kg^{-1} decreased locomotion, as evidenced by reduced 'move in contact' and increased 'stop isolated' time, diminishing social interaction in both WT and *Fmr1* KO mice (Figures 4, S7). Acute administration of the highest dose had sedative effects, while subchronic administration showed variable enhancement of nose contacts and huddling behaviours in WT mice (Figure 4).

The pharmacokinetics of RO6893074 following a single intraperitoneal dose of 5 mg.kg^{-1} and 50 mg.kg^{-1} in mice, indicated an average maximum plasma concentration (Cmax) of approximately 220 ng.mL^{-1} and 7000 ng.mL^{-1}, with a time to reach Cmax (Tmax) of 0.5 hours and 0.84 hours, respectively. The area under the plasma concentration-time curve from time 0 to infinity (AUC_0-∞) was 581 and 16400 ng.h.mL^{-1}, respectively. The elimination clearance (CL = Dose/AUC) was dose-dependent. Based on free plasma exposure of 6.3% (considering the compound is not a substrate for mouse P-glycoprotein and has good permeability) and *in*

vitro V_{1A} binding, the corresponding brain V_{1A} receptor occupancy was estimated to be approximately 49% and 96% at doses of 5 $mg.kg^{-1}$ and 50 $mg.kg^{-1}$, respectively. Administration at doses of 10 $mg.kg^{-1}$ and 100 $mg.kg^{-1}$ is expected to yield approximately 65% and 98% occupancy, respectively. Biological effects of V_{1A} blockade are expected to be detectable between 70 to 90% receptor occupancy (Grimwood and Hartig, 2009). Higher exposure may lead to inhibition of off-target receptors, inducing non-specific side effects, as observed in WT mice (Figure 4A).

In conclusion, selective OTR agonists TGOT at 20 $\mu g.kg^{-1}$ or RO6958375 at 0.03 and 0.06 $mg.kg^{-1}$ restored social impairments in *Fmr1* KO mice, while TGOT at 40 $\mu g.kg^{-1}$ reduced sociability in WT mice. RO6958375 displayed the most favourable dose effect with fewer side effects. The V_{1A} antagonist RO6893074 showed some beneficial effects in *Fmr1* KO mice at 50 $mg.kg^{-1}$, resulting in 96% V_{1A} receptor occupancy, although these effects were not sustained with subchronic administration.

DISCUSSION

In our study, we evaluated the efficacy, potency and selectivity of various ligands targeting oxytocin and vasopressin receptors in neuronal heterologous cells. Despite similar binding affinities (Busnelli et al., 2013), OT and AVP exhibited distinct efficacy and potency across their receptors. They primarily recruit miniGq and β-arrestins at OTR, V_{1A}, and V_{1B} receptors, while the V_2 receptor also activates miniGs. These findings are in line with previous studies (Birnbaumer, 2000; Busnelli et al., 2012, 2013; Heydenreich et al., 2022). None of the receptors coupled with miniGi proteins or mediated cAMP inhibition in our assays, which contrasts with previous reports for OTR or V_2 receptors (Strakova and Soloff, 1997; Busnelli et al., 2012; Heydenreich et al., 2022). The lower affinity of the chimeric miniGi protein may explain these differences and may also account for the variations observed in the calcium assay. Previous studies identified an association between $G\alpha_{i3}$ and OTR in rat myometrium and CHO cells (Strakova and Soloff, 1997; Strakova et al., 1998) and described conformational changes between $G\alpha_{i/o}$ and $G_{\beta\gamma}$ subunits or OTR fused to YFP and G_γ upon OT stimulation in HEK293 cells (Busnelli et al., 2012). These findings imply that OTR could signal through $G_{\beta\gamma}$ release, as previously shown (Camps et al., 1992), although this was not detected in our assays. While β-arrestin-1 and -2 recruitment was comparable across receptors and ligands, we cannot exclude the possibility of distinct conformational changes between the two β-arrestins (Haider et al., 2022). Isotocin, mesotocin or vasotocin displayed pharmacological profiles similar to OT or AVP, respectively, and did not act as biased agonists on the four receptors. Surprisingly, kB7-OT and carbetocin failed to activate OTR in our assays, except for carbetocin on V_2 receptors, which contrasts with previous studies (Koehbach et al., 2013; Passoni et al., 2016). This difference may be attributed to lower receptor expression in HEK293A cells and distinct signalling assays (miniGq *vs.* $G\alpha$-G_γ BRET assays). We identified

297 TGOT and RO6958375 peptides as miniGq-biased agonists for OTR and V_2 receptors — a
298 profile previously reported only for TGOT on OTR (Busnelli et al., 2013). Given that V_2 is not
299 expressed in neurons or glia and does not participate in social behaviours (Ostrowski et al.,
300 1992; Kato et al., 1995), the administration of these agonists *in vivo* primarily targets social
301 inputs regulated by OTR in the brain. Intranasal administration of OT and AVP showed limited
302 efficacy in improving social impairments in *Fmr1* KO mice. Our results align with previous
303 studies (Lindenmaier et al., 2022; Pan et al., 2022) and reflect the outcomes of clinical trials
304 where intranasal administration did not consistently yield therapeutic effects in individuals
305 with ASD (Guastella et al., 2010; Bernaerts et al., 2020; Annamneedi et al., 2023; Daniels et
306 al., 2023). The therapeutic potential of OT may be diminished by the activation of both
307 oxytocin and vasopressin receptors, despite OT activating V_{1A} receptors to a lesser extent *in*
308 *vitro*. Potential hetero-oligomerization between OTR and V_{1A} (Terrillon et al., 2003) or V_{1B}
309 receptors could also impact *in vivo* outcomes. In addition, OT has poor blood brain barrier
310 penetration even following intranasal administration, resulting in low brain exposure and high
311 interindividual variability (Leng et al., 2022).
312 Conversely, selective OTR agonists TGOT or RO6958375 improved social interactions in WT
313 and *Fmr1* KO mice at low doses. This supports the hypothesis that unselective activation of
314 vasopressin receptors by endogenous OT may counteract the pro-social effects of OTR
315 activation. The combination of OT administration with behavioural interventions appears
316 more effective in reducing social deficits (Ford and Young, 2022; Daniels et al., 2023; Pantouli
317 et al., 2024). Our experimental approach, which exposed mice to repeated social interactions
318 with unfamiliar mice, may have enhanced the effectiveness of TGOT and RO6958375.
319 Longitudinal studies could provide more comprehensive insights into the persistence of
320 therapeutic effects, including post-treatment outcomes. TGOT and RO6958375 showed

distinct effects in *Fmr1* KO and WT mice. RO6958375 administration consistently improved social interactions in *Fmr1* KO mice without affecting WT sociability, suggesting a more favourable profile than intranasal TGOT. The different administration routes (intranasal *vs.* subcutaneous) may also influence brain exposure and reduce interindividual exposure variability.

The two OTR agonists, characterised by lower β-arrestin recruitment efficiency and potency *in vitro* compared to OT, may provide sustained OTR signalling with limited desensitisation and internalisation, offering a crucial therapeutic advantage for chronic treatment. Differences between these OTR agonists may be attributed to their distinct kinetic profiles or efficacy *in vitro*. Ligands that are selectively biased towards G protein or β-arrestin pathways have been shown to optimise therapeutic effects for other neurological disorders while minimising potential side effects of the other signalling pathways (Park et al., 2016; Lee et al., 2021; Kolb et al., 2022).

In contrast, the acute selective blockade of the V_{1A} receptor with RO6893074 was less beneficial for social approach in *Fmr1* KO mice than OTR agonists, but did acutely increase nose contact and huddling. The supratherapeutic intraperitoneal dose of 100 $mg.kg^{-1}$ affected locomotion, likely due to off-target effects. This suggests that blocking V_{1A} receptors may elicit different behavioural outcomes than OTR activation. Therefore, combining RO6893074 with an OTR agonist could potentially enhance therapeutic outcomes for social features.

Targeting the OTR with low doses of selective agonists improves social interactions in *Fmr1* KO mice, while eliciting only limited side effects in WT mice. These findings open new avenues for developing OTR-targeted therapies for ASD. Although challenging, the development of OTR positive allosteric modulators enhancing OTR signalling in brain regions where OT is endogenously released holds promise. Additionally, $G\alpha_{q/11}$- or β-arrestin-biased agonists that

induce signalling bias towards specific pathways and limit side effects may be effective therapies for ASD. Understanding the precise contributions of each receptor to social interaction, as well as their expression levels and the role of peptides remains crucial. Our study offers new insights into OTR activation and V_{1A} inhibition on sociability. Future research should investigate the effects of selective V_{1A} agonists (Andrés et al., 2002; Marir et al., 2013) or the OTR antagonist atosiban, as well as the role of V_{1B} receptors, which have more restricted expression in the brain (Young et al., 2006; Stevenson and Caldwell, 2012), to elucidate their contributions. A limitation of this study is the lack of direct measurement of mouse brain exposure for the tested compounds. This data would provide more accurate estimates of brain receptor occupancy and the relative contributions of G-protein signalling versus β-arrestin recruitment.

While our study focused on social features, assessing effects on stereotyped behaviours, cognitive flexibility or anxiety would provide a more comprehensive evaluation of treatment efficacy. Testing OTR agonists in mouse models using a molecular stratification approach based on specific molecular markers across models mimicking the autism spectrum (Gora et al., 2024), may enhance translatability and facilitate the development of personalised medicines for individuals with ASD.

MATERIALS AND METHODS

Compounds

For *in vitro* assays, drug powders of oxytocin (OT; 1910, Tocris Bioscience™, UK), (Arg^{8})-vasopressin (AVP; 2935, Tocris Bioscience™, UK), (Butyryl^{1},Tyr(Me)^{2})-1-Carbaoxytocin (carbetocin; 4040269, Bachem, Switzerland), (Ser^{4},Ile^{8})-oxytocin (isotocin; 4030890, Bachem, Switzerland), (Ile^{8})-oxytocin (mesotocin; 4030888, Bachem, Switzerland), (Arg^{8})-vasotocin (vasotocin; 4100576, Bachem, Switzerland), (Thr^{4},Gly^{7})-oxytocin (TGOT; 4013837, Bachem, Switzerland), RWJ22164 (atosiban; 4065438, Bachem, Switzerland), (Gly^{5},Thr^{7},Ser^{9})-oxytocin (kB7-OT; 4144391, Bachem, Switzerland), L-371,257 (2410, Tocris Bioscience™, UK), RO6958375 OTR peptide agonist (c[Gly-Tyr-Ile-GIn-Asn-Glu]-*trans*-4-fluoro-Pro-Leu-Gly-NH_2, Roche pharmaceutical, Switzerland) (Janz et al., 2023) and RO6893074 V_{1A} chemical antagonist (*trans*-2-(4-(4-(4-chlorophenyl)-5-methyl-4*H*-1,2,4-triazol-3-yl)cyclohexyloxy)pyridine, Roche pharmaceutical, Switzerland) were dissolved at 10^{-2} M in 100% DMSO (20-139, Sigma-Aldrich, USA), aliquoted and stored at -20°C until further use. On the testing day, all compounds were diluted in PBS 1X + 10 mM HEPES (CSTHEP00-0P, Eurobio, France) at 4°C and tested alone. In addition for their antagonist effects, atosiban, L-371,257 and RO6893074 V_{1A} antagonists were diluted at EC_{80} (concentration reaching 80% of maximal efficacy) in 10^{-6} M of OT for OTR or in 10^{-6} M of AVP for V_{1A} and V_{1B} or 10^{-8} M for V_2. Coelenterazine luciferase substrate (R3078C, Interchim, France) was protected from light exposure and stored at 1 mM in 100% ethanol (64-17-5, Carlo Erba Reagents, France) and then diluted to 5 µM final in PBS 1X.

For *in vivo* assays, OT, AVP and TGOT were diluted at 20 and 40 µg.kg^{-1} in NaCl 0.9% (190/12604022/1021, Braun, Germany), corresponding to low and moderate doses (0.03 and 0.06 IU) at 4°C and stored in aliquot for daily use at −20°C (vehicle: NaCl 0.9%). RO6958375

386 and RO6893074 compounds were formulated at Roche Pharmaceutical at 0.03, 0.06 and 0.12
387 mg.kg^{-1} in PBS 1X for subcutaneous administration of RO6958375 OTR peptide agonist
388 (vehicle: PBS 1X), and at 25, 50 and 100 mg.kg^{-1} in 0.1% polysorbate Tween-80, 0.21% citric
389 acid monohydrate, 0.8% sodium chloride, sodium hydroxide 1N at pH 7 diluted in water for
390 intraperitoneal injection of RO6893074 V_{1A} small molecule antagonist (vehicle: 0.1%
391 polysorbate Tween-80, 0.21% citric acid monohydrate, 0.8% sodium chloride, sodium
392 hydroxide 1N at pH 7) and stored in aliquot for daily use at 4°C until further use.
393
394 ***Cell culture***
395 Neuro-2a mouse neuroblastoma (Neuro-2a; CCL-131™, RRID:CVCL_0470, ATCC, USA) cells
396 were regularly tested for negative mycoplasma contamination were cultured in Eagle's
397 Minimal Essential Medium (EMEM; CM1MEM40-01, Eurobio, France) supplemented with
398 10% (v/v) foetal bovine serum (CVFSVF00-01, Eurobio, France), 1% penicillin/streptomycin
399 (100 U.mL^{-1}, 100 µg.mL^{-1}, respectively; 15140-122, Eurobio, France) and 1% L-glutamine (2
400 mM; CSTGLU00-0U, Eurobio, France), and maintained at 37°C with 5% CO_2. When reaching
401 90% confluency, cells were washed with PBS 1X (CS1PBS01K-BP, Eurobio, France) followed by
402 trypsin (0.5 g.L^{-1}, L-EDTA 0.2 g.L^{-1}, without phenol red; CEZTDA00-0U, Eurobio, France)
403 treatment. After cell counting, cells were transiently transfected in suspension using the

Metafectene Pro transfection reagent (T040-5.0, BioNTex Laboratories, Germany) according to the manufacturer's protocol.

G protein, β-arrestin recruitment and internalisation using Bioluminescence Resonance Energy Transfer (BRET) assays

In 96-well plates (30196, SPL Life Sciences, Korea), around 40,000 Neuro-2a cells per well were transiently co-transfected with the mouse oxytocin receptor cDNA *Oxtr* or mouse vasopressin *Avpr1a, Avpr1b* subcloned using HindIII and XhoI in pcDNA3 plasmid or with the *Avpr2* receptors in pcDNA3.1(+) plasmid, fused in their C-terminus to the BRET donor *Renilla reniformis* luciferase (RLuc8) at 50 ng/well, along with BRET acceptor sensors containing a yellow fluorescent proteins (YFP, Venus or YPET) at 50 ng/well each. For the miniG protein recruitment, we used the pNluc–C1 vector encoding the miniG proteins fused in their N-terminus to the Nuclear Export Signal (NES) to avoid their transport to the nucleus; NES-Venus-mG$_s$, NES-Venus-mG$_i$ or NES-Venus-mG$_q$ (provided by Pr Nevin A. Lambert, Augusta, GA, USA) (PMID: 29523687), namely miniGs, miniGi and miniGq, respectively. MiniGs proteins are engineered Gα subunits with modifications such as the exclusion of the α-helical domain, a shortened N-terminus which removes both membrane anchors and the G$_{\beta\gamma}$-binding surface, specific mutations to enhance *in vitro* protein stability and a mutation in the C-terminal 5-helix to stabilise receptor–miniG complexes even in the presence of guanine nucleotides. For miniGq and miniGi, the five C-terminal amino acids of miniGs, which form the main receptor binding site and are key determinants of coupling specificity, were replaced with those of Gα$_q$, necessitating three mutations. For miniGi, 9 mutations were done into the Gα5 helix to change the coupling specificity from Gα$_s$ to Gα$_i$ (Nehmé et al., 2017; Wan et al., 2018). For β-arrestin recruitment, we used YPET-β-arrestin-1 or YPET-β-arrestin-2 (provided by Dr M.G.

Scott, Paris, France) (Kamal et al., 2009) encoded in pcDNA3.1 plasmid. For internalisation experiments, the yellow fluorescent protein YPET was fused to the CAAX box of KRas protein and the FYVE domain of endofin, according to (Lee et al., 2005; Namkung et al., 2016), namely YPET-CAAX addressed at the plasma membrane or YPET-FYVE addressed at the endosome membrane, respectively. Their sequences were synthesised at Twist Bioscience and subcloned in pcDNA3.1 plasmid by recombination between HindIII and XhoI restriction sites. For cAMP assay, pcDNA3.1(+) encoding untagged murine receptors and the CAMYEL (provided by Dr Lily Jiang, Texas, USA) (Jiang et al., 2007), a cAMP EPAC sensor (YFP-Epac-RLuc8) were co-transfected at 50 ng/well.

48 hours after transfection, Neuro-2a cells were starved for 4 hours in phenol red-free DMEM (21063-029, Gibco, France) at 37°C in 5% CO_2. Cells incubated with coelenterazine substrate (5 µM) were first measured for 5 minutes at 480 ± 20 nm and 530 ± 25 nm (Mithras2 LB 943 with the Mikrowin 2010 software, Berthold Technologies GmbH & Co., Germany). Then, cells were rapidly stimulated with the different agonists at 3.10^{-5} M, 10^{-5} M, 10^{-6} M, 10^{-7} M, 10^{-8} M, 10^{-9} M, 10^{-10} M diluted in PBS 1X and HEPES 10 mM final, or PBS 1X and HEPES 10 mM alone for the baseline, then 96-well plates were recorded for 30 minutes. When testing the effect of the antagonists, they were tested at the same concentration as agonists and in presence of OT at EC_{80} for OTR or AVP at EC_{80} for the V_{1A}, V_{1B} or V_2 receptors. For cAMP production and inhibition BRET assays, compounds were tested in absence or presence of forskolin at 5.10^{-6} M (F6886, Sigma-Aldrich, USA), respectively. Each condition was performed in triplicate

within the same 96-well plate, and all experiments were independently repeated at least three times.

Calcium mobilisation assays using luminescence

In 6-well plates (353046, Corning, USA), around 400,000 Neuro-2a cells per well were plated 24 hours at 37°C with 5% CO_2 before transfection. Then, cells were transiently transfected with the untagged mouse oxytocin (*Oxtr*) or vasopressin (*Avpr1a, Avpr1b or Avpr2*) receptor cDNAs subcloned using HindIII and XhoI in the pcDNA3.1(+) plasmid at 1 µg/well and pPD16 vector encoding the calcium-sensitive bioluminescent protein aequorin from the jellyfish *Aequorea victoria* jellyfish (GFP-aequorin provided by Dr Bertrand Lambolez, Paris, France) at 2 µg per well (Drobac et al., 2010). 48 hours after transfection, Neuro-2a cells were Ca^{2+}-deprived for 4 hours at 37°C with 5% CO_2 using the Hank's Balanced Salt Solution (CS1SSH22-0U HBSS; Eurobio, France) with no calcium or phenol red and containing 5 µM coelenterazine in the dark. Subsequently, cells were harvested and centrifuged at 500g for 5 minutes. Cell pellets were resuspended in around 2.10^6 cells.mL^{-1} of HBSS with 1.26 mM of calcium (CS1SSH23-0U; Eurobio, France) and 5 µM coelenterazine, and incubated for one hour at 37°C in the dark. OT and AVP ligands were diluted in HBSS with 1.26 mM of calcium across at 10^{-5}M, 10^{-6}M, 10^{-7}M, 10^{-8}M, 10^{-9}M, 10^{-10}M, 10^{-11}M, 10^{-12}M final concentrations on ice, and HBSS with 1.26 mM of calcium alone for baseline. Ten µL per well of each concentration of ligand (5X) was loaded in duplicate into a 384-well plate and 40 µL of cells (around 40,000 cells per

468 well) were injected into each well. Luminescence of calcium-bound aequorin signals was
469 continuously measured for 25 seconds.
470
471 ***In vitro data modelling and analysis***
472 *BRET and calcium assays*
473 The 530 nm/480 nm BRET ratios were normalised to the initial unstimulated BRET ratio and
474 then computed into "Induced BRET" values by subtracting the control (PBS) ratio at each
475 measurement time point. Then, the area under curves (AUC) were estimated over the 30-
476 minute induced BRET measurements or directly for calcium assays over the 25-second
477 measurements for each receptor, ligand and concentration combination to study the
478 concentration–response relationship. Concentration-response curves were modelled with a
479 four-parameters log-logistic equation, with E_{min} (minimal response), E_{max} (maximal response),
480 EC_{50} (concentration to reach $E_{max}/2$) and h (sigmoidicity coefficient). Concentration-response

curve values were then normalised to the E_{max} value of the reference ligand for each receptor (i.e. OT for OTR and AVP for V_{1A}, V_{1B} and V_2 receptors).

Ligand bias calculation has been done according to GPCR ligand bias guidelines (Kolb et al., 2022). For each normalised dose-response curve, we computed a transduction coefficient $\log(\tau/K_A)$ defined by the following equation:

$$\text{response} = \frac{E_m}{1 + \exp\left\{ n \ln\left[1 + \frac{\exp(\beta_1)}{[A]} \right] - n\beta_2 \right\}}$$

Where $\beta_1 = \ln(K_A)$ and $\beta_2 = \ln(\tau)$ and $\log(\tau/K_A) = (\beta_2 - \beta_1)/\ln(10)$.

This composite parameter reflects the affinity and efficacy of the ligand-receptor interaction and the induction of downstream signalling pathways measured by each assay (Kenakin et al., 2012).

<u>*Mathematical modelling of ß-arrestin-2 recruitment and Internalisation assays*</u>

In this section, we detail the kinetic analysis on β-arrestin-2, FYVE and CAAX induced BRET signals. This methodology was independently applied for each murine receptor OTR, V_{1A}, V_{1B} and V_2, and each endogenous ligand OT and AVP.

I) Kinetic model

We adapted and extended the methodology presented in (Hoare et al., 2020). More precisely, we used the following kinetic reaction network model :

(1) $R \rightarrow RAB \rightarrow RI \rightarrow R$

where *R* denotes the unbound membrane receptor, *RAB* denotes the receptor-agonist-β-arrestin-2 complex, and *RI* denotes the internalised receptor. We assume fast binding kinetics between the agonist and the receptor and that the agonist is in excess compared to the receptor (Hoare et al., 2020). We further assume that the free β-arrestin-2 is in excess

compared to the receptor-agonist complex, thus its depletion can be neglected. As a result, the model **(1)** is a first-order kinetic reaction network whose dynamics is represented by the linear three-dimensional ordinary differential equation (ODE):

$$\begin{aligned} \frac{d}{dt}R &= -k_\tau \frac{A}{A+K_D}R + k_{rec}RI \\ \frac{d}{dt}RAB &= k_\tau \frac{A}{A+K_D}R - k_{int}RAB \\ \frac{d}{dt}RI &= k_{int}RAB - k_{rec}RI \end{aligned} \quad \textbf{(2)}$$

where A (mol) is the agonist concentration, K_D (mol) is the binding affinity of the agonist and the receptor, k_τ (min^{-1}) is β-arrestin-2 recruitment rate, k_{int} (min^{-1}) is the internalisation rate and k_{rec} (min^{-1}) is the recycling rate. The initial condition associated with system **(2)** is:

$R(0)=R_{tot}, RAB(0)=0, RI(0)=0,$

where R_{tot} (mol) is the total quantity of receptors.

II) Model fitting and parameter estimation

The CAAX induced BRET ratio was taken as proportional to the loss of receptors at plasma membrane, $R\text{-}R_{tot}$, the β-arrestin-2 induced BRET ratio was taken as proportional to the quantity of receptor-agonist-β-arrestin-2 complex *RAB*, and the FYVE induced BRET ratio is

taken proportional to the quantity of internalised receptor *RI*, with standard gaussian measurement errors with unknown variance, as follows :

(3) $CAAXinducedBRETratio = y_1 = k_{bret,1} \cdot (R-R_{tot}) + \varepsilon_{0,\sigma 1}$

$Barr_2inducedBRETratio = y_2 = k_{bret,2} \cdot RAB + \varepsilon_{0,\sigma 2}$

$FyveinducedBRETratio = y_1 = k_{bret,3} \cdot RI + \varepsilon_{0,\sigma 3}$

where $k_{bret,1}$, $k_{bret,2}$ and $k_{bret,3}$ are proportional constant, and $\varepsilon_{0,\sigma 1}$, $\varepsilon_{0,\sigma 2}$ and $\varepsilon_{0,\sigma 3}$ are standard centred standard gaussian distribution of variances σ_1, σ_2 and σ_3, respectively.

As detailed in (Raue et al., 2013), model adimentionalisation and reparameterisation is a prerequisite for a successful and meaningful estimation. To that, we divided each variable by R_{tot} and transformed the system **(2)** into the following equivalent system:

(4)
$$
\begin{aligned}
\frac{d}{dt}x_1 &= k_{int}\left(-\overline{k_\tau}\frac{A}{A+K_D}x_1 + \overline{k_{rec}}x_3\right)\\
\frac{d}{dt}x_2 &= k_{int}\left(\overline{k_\tau}\frac{A}{A+K_D}x_1 - x_2\right)\\
\frac{d}{dt}x_3 &= k_{int}\left(x_2 - \overline{k_{rec}}x_3\right)\\
x_1(0) &= 1, \quad x_2(0) = 0, \quad x_3(0) = 0\\
y_1 &= \overline{k_{bret,1}}(x_1 - 1) + \varepsilon_{0,\sigma_1}\\
y_2 &= \overline{k_{bret,2}}x_2 + \varepsilon_{0,\sigma_2}\\
y_3 &= \overline{k_{bret,3}}x_3 + \varepsilon_{0,\sigma_3}
\end{aligned}
$$

where, $\overline{k_\tau} = \frac{k_\tau}{k_{int}}$, $\overline{k_{rec}} = \frac{k_{rec}}{k_{int}}$, $\overline{k_{bret,1}} = \frac{k_{bret,1}}{R_{tot}}$, $\overline{k_{bret,2}} = \frac{k_{bret,2}}{R_{tot}}$, $\overline{k_{bret,3}} = \frac{k_{bret,3}}{R_{tot}}$,

In the ODE system **(4)**, k_{int} has (min^{-1}) unit, *A* is the (known) agonist concentration, K_D has molar unit, and all other constants are unitless. This model has a total of 10 unknown parameters whose search intervals are given in Table S3.

We solved the system of ODE **(4)** using the *AMICI* package (Fröhlich et al., 2021) and performed parameter estimation following the maximum likelihood approach. We specified the parameter estimation problem following the Petab (Schmiester et al., 2021) format and solved it using the pyPESTO toolbox (Schälte et al., 2023), in Python. Parameter confidence

intervals were determined using the profile likelihood approach, implemented in pyPESTO. In addition, we verified that the parameter estimation problem is theoretically well-posed using the *StructuralIdentifiability* package in Julia (Dong et al., 2023), which shows that all parameters of model **(4)** are structurally identifiable given data on y_1, y_2, y_3 for at least two agonist doses. We report in Table S3 maximum likelihood estimates with their profile-based confidence intervals.

III) Model selection

The model fitting procedure reveals over-fitting issues for model **(4)** and for some of the agonist-receptor combinations, resulting in practical parameter unidentifiability and large confidence parameter intervals. Further analyses revealed large uncertainties in the $\overline{k_{rec}}$ parameter, suggesting that a model without recycling could equally fit the data (k_{rec} = 0).

Therefore, we asked whether the following submodel could be more suitable l to describe the data:

(5) *R→RAB→RI*

Using the same methodology as in section I and II, we obtained the following reduced model:

$$
\begin{aligned}
\frac{d}{dt}x_1 &= k_{int}\left(-\overline{k_\tau}\frac{A}{A+K_D}x_1\right)\\
\frac{d}{dt}x_2 &= k_{int}\left(\overline{k_\tau}\frac{A}{A+K_D}x_1 - x_2\right)\\
\frac{d}{dt}x_3 &= k_{int}\overline{k_{bret,3}}x_2\\
x_1(0) &= 1, \quad x_2(0) = 0, \quad x_3(0) = 0\\
y_1 &= \overline{k_{bret,1}}(x_1 - 1) + \varepsilon_{0,\sigma_1}\\
y_2 &= \overline{k_{bret,2}}x_2 + \varepsilon_{0,\sigma_2}\\
y_3 &= x_3 + \varepsilon_{0,\sigma_3}
\end{aligned}
\qquad \textbf{(6)}
$$

where, $\overline{k_\tau} = \frac{k_\tau}{k_{int}}$, $\overline{k_{bret,1}} = \frac{k_{bret,1}}{R_{tot}}$, $\overline{k_{bret,2}} = \frac{k_{bret,2}}{R_{tot}}$, $\overline{k_{bret,3}} = \frac{k_{bret,3}}{R_{tot}}$

In the ODE system **(6)**, k_{int} has (min^{-1}) unit, A is the (known) agonist concentration, K_D has molar unit, and all other constants are unitless. This reduced model has a total of 9 unknown parameters whose search intervals are given in Table S3.

We performed parameter estimation of model **(6)** using the same methodology for model **(4)**. We report in Table S3 maximum likelihood estimates with their profile-based confidence intervals. For each receptor-agonist combination we performed a model selection procedure to select either model **(4)** or model **(6)**. We report in Table S3 standard likelihood ratio p-values (α=0.05) and AIC and BIC criteria.

Animals

All mouse breeding, care and experimental procedures were in accordance with the European and French Directives and approved by the local ethical committee CEEA Val de Loire N°19 and the French ministry of teaching, research and innovation (APAFIS #18035-

2018121213436249). Following heterozygous breeding scheme, independent cohorts of *Fmr1* KO (provided by Rob Willensem (Mientjes et al., 2006)) and WT mice were generated from a minimum of 3 different homozygous non-inbred couples maintained on a mixed 50%-50% C57BL/6J;129S2 background in the same breeding room of the animal facility. Mice were outcrossed with fresh mixed backgrounds every 5-10 generations, and between them, with WT mice from other lines, to prevent inbreeding and ensure consistency across independent batches. This *in vivo* experimental model in mice replicates aspects of the human Fragile X syndrome (Kat et al., 2022). Two months old naive males and females from *Fmr1* KO (n = 235, 107 males and 128 females) and WT (n = 188, 84 males and 104 females) animals were raised in groups of 2-4 animals on a 12-hour light/dark regular cycle, with food and water *ad libitum* and controlled temperature (21°C) and humidity (50%) in conventional health housing status, exempt from any monitored viral, bacterial, mycoplasma, fungi, parasites or pathological lesions, except detected mouse norovirus and *helicobacter spp*. Cages of WT and *Fmr1* KO mice were randomly allocated by an experienced experimenter to a treatment to obtain at least 8 animals (4 males and 4 females) per group.

Mouse intraperitoneal single dose pharmacokinetic with RO6893074 and V_{1A} Receptor occupancy calculation

An exploratory single-dose pharmacokinetic study in three C57BL/6J male mice (Charles River) was conducted with RO6893074 V_{1A} small molecule antagonist following intraperitoneal administration at the doses of 5 $mg.kg^{-1}$ and 50 $mg.kg^{-1}$. The compound was formulated as a microsuspension in HPMC / DOSS (1.25% / 0.1%) / Parabens, with a pH of 6. Blood samples were collected at 6 time points: 0.25, 0.5, 1, 3, 5, 7 hours after administration and the

compound was detected using mass spectrometry. Pharmacokinetic parameters were derived from the plasma concentration versus time profile.

Using *in vitro* plasma free fraction (fup = 6.3%) and *in vitro* V_{1A} binding data (mouse V_{1A} Ki = 39 nM, n = 3), the following Emax equation was used to calculate receptor occupancy at Cmax (assuming competitive inhibition):

$$\text{Receptor occupancy} = B\max \times \frac{Cp \times fup}{Ki + Cp \times fup} = B\max \times \frac{\frac{Cp \times fup}{Ki}}{1 + \frac{Cp \times fup}{Ki}}$$

where Bmax is the maximum binding, assumed to be 100%, Cp is the plasma concentration of the compound, fup is the free fraction in plasma, and Ki represents *in vitro* binding to the receptor.

Drug administration

WT and *Fmr1* KO mice were administered every mornings for 8 consecutive days from day 0 (acute) to day 7 (subchronic) with OT, AVP or TGOT (20 or 40 µg.kg^{-1}, 0.2 mL.kg^{-1}, intranasally, 15 minutes prior to behavioural tests), RO6958375 OTR agonist (0.03, 0.06 or 0.12 mg.kg^{-1}, 10 mL.kg^{-1}, subcutaneously, 30 minutes prior to behavioural tests) or RO6893074 V_{1A} antagonist (25, 50 or 100 mg.kg^{-1}, 10 mL.kg^{-1}, intraperitoneally, 30 minutes prior to behavioural tests) based on previous studies (Peñagarikano et al., 2015; Janz et al., 2023) and Roche recommendations, along with their respective vehicles (for OT, AVP or TGOT: NaCl 0.9%, intranasally, 0.2 mL.kg^{-1}; for RO6958375: PBS 1x, intraperitoneally, 10 mL.kg^{-1}; for RO6893074: 0.1% polysorbate Tween-80, 0.21% citric acid monohydrate, 0.8% sodium chloride, sodium hydroxide 1N at pH 7, subcutaneously, 10 mL.kg^{-1}). For intranasal administration, each drop was placed alternately to each nostril until the animal aspirated the drop into its nasal cavity. As both TGOT and RO6958375 OTR agonists can activate the V_2

receptor, we carefully monitored the mouse weight, which remained stable, for potential diuretic effects of V_2 receptor activation.

Social interactions using the Live Mouse Tracker

One week before the behavioural experiments, RFID chips (APT12 PIT Tag, Biomark, USA) were inserted under the skin on the lateral and ventral side of the abdomen in *Fmr1* KO and WT mice under Isoflurane gas anaesthesia (FR/V/4397332 3/2021, Isoflurin®; Axience SAS, France) and a Procaine local anaesthetic (FR/V/6012689 8/2013, Procamidor®; Axience SAS, France) at 40 µg/10g^{-1} subcutaneously 10 min at the insertion site. All behavioural tests were carried out, when possible, in the morning, to avoid any circadian cycle effect, in a dedicated quiet room and a dim light intensity of 15 lux. Males were always tested before females to prevent any sexual olfactory bias. The Live Mouse Tracker (LMT) (LMT_SOURIS, Rodent Phenotyping Toolkit, France (de Chaumont et al., 2019)) is a reproducible and automatic tracking device that identifies in real time over 30 behavioural parameters of reciprocal social interaction using constant RFID detection and an infrared–depth sensing camera. Two mice matched by sex, age, genotype and treatment that had never met before were placed in the LMT for 10 min at 15 lux in a transparent red Plexiglass open field (50 x 25 x 30 cm). Floors were covered with a thin layer of fresh wood litter to favour normal locomotion, well-being and reduced anxious-like behaviours. Social interaction tests were performed 3 days before the treatment (D-3), the first day (D0) and the last day (D7) of treatment (acute *vs.* subchronic effects). Multi-behavioural parameters were analysed, such as individual events (moving isolated, stopped isolated, rearing), dyadic state events (moving in contact, following, stopped in contact, contact side by side, nose-to-nose contact, nose-anogenital contact), locomotion (% of time moving) and anxious-like behaviours (stretch-attend posture). SQLIte

databases containing the coordinates of each mouse and movies were generated for each run of interaction. All individual behavioural parameters were extracted using Python scripts (github.com/fdechaumont/lmt-analysis version v1.0.6). “Nose contacts” or “huddling” were the sum of nose-to-nose and nose-to-anogenital region contacts, or contact side by side in same or in opposite directions, respectively. For each mouse line, mice injected with vehicles were used as control of those injected with the different drug compounds at D0 and D7. While experimenters were not blinded to the conditions during the tests to prevent any exchange of mice, scoring was conducted automatically for reciprocal social interaction by the Live Mouse Tracker. All animal criteria have been reported in agreement with the ARRIVE guidelines (Kilkenny et al., 2010). The SAL, PBS and VEH WT group consisted of independent batches of WT mice, serving as the controls for each mouse line or treatment condition and batch.

Statistical analysis

Computation and subsequent statistical analysis were performed using R software (version 4.4.0). Parameter values of the concentration-effect curves were estimated by a nonlinear mixed-effect model (population approach) using Monolix Suite 2024R1 (Lixoft, Antony, France). Concentration-Effect curve parameters E_{max}, $\log(EC_{50})$ and $\Delta\log(\tau/Ka)$ were compared to the parameters of the receptor referent-ligand with a Student t-test, taking into account the mean and standard deviation estimated by the population approach and the number of experimental replicates.

No animal outliers were removed from the analysis. For the Live Mouse Tracker data analysis, Kruskal-Wallis tests were conducted using the rstatix package (Alboukadel Kassambara,

2023)(R package version 0.7.2) followed by Dunn's *post hoc* tests. Sex differences were analysed only before treatment allocation, as sample sizes were too small for comparison.

Data availability statement

All *in vitro* and *in vivo* raw data, means and statistics are available in supplementary Tables. Codes and configuration files are available on the research.data.gouv.fr. Movies of behavioural experiments are available upon request.

AUTHOR CONTRIBUTIONS

PS and ChG provided materials and an unpublished tool compound; CG, ChG and LPP designed the experiments; CG, LD, EP and LPP performed the experiments and contributed to the data collection; CG, LD, ChG, RY, NA and LPP contributed to the interpretation of data; RY and NA performed all data integration, modelling and statistical analysis; PDP performed the brain receptor occupancy modelling; CG and LPP wrote the original drafts; CG, LD, EP, PS, PDP, ChG, RY, NA and LPP reviewed and edited the manuscript; LPP contributed to the funding acquisition, project conceptualization and supervision.

ABBREVIATIONS

ASD autism spectrum disorders

AVP Arginine vasopressin

Avpr1A mouse vasopressin V_{1A} receptor gene

Avpr1B mouse vasopressin V_{1B} receptor gene

Avpr2 mouse vasopressin V_2 receptor gene

AVPR1A human vasopressin V_{1A} receptor gene

AVPR1B human vasopressin V_{1B} receptor gene

AVPR2 human vasopressin V_2 receptor gene

BORIS behavioural observation research interactive software

BRET bioluminescence resonance energy transfer

DMEM dulbecco's modified eagle medium

EMEM eagle's minimal essential medium

FMR1 fragility mental retardation 1

HBSS hank's balanced salt solution

HEK293A human embryonic kidney 293A

kB7-OT [Gly^5,Thr^7,Ser^9]-Oxytocin

KO knockout

LMT live mouse tracker

Neuro-2a mouse neuroblastoma Neuro-2a cell line

OT oxytocin

OTR oxytocin receptor

Oxtr mouse oxytocin receptor gene

OXTR human oxytocin receptor gene

RLuc8 sea pansy renilla reniformis luciferase

SAP stretch-attend postures

TGOT [Thr4,Gly7]OT

WT wild-type

REFERENCES

Alboukadel Kassambara (2023). rstatix: Pipe-Friendly Framework for Basic Statistical Tests.

Alexander, S.P., Christopoulos, A., Davenport, A.P., Kelly, E., Mathie, A., Peters, J.A., et al. (2021). THE CONCISE GUIDE TO PHARMACOLOGY 2021/22: G protein-coupled receptors. Br. J. Pharmacol. *178 Suppl 1*: S27–S156.

American Psychiatric Association (2013). Diagnostic and Statistical Manual of Mental Disorders (American Psychiatric Association).

Andrés, M., Trueba, M., and Guillon, G. (2002). Pharmacological characterization of F-180: a selective human V(1a) vasopressin receptor agonist of high affinity. Br. J. Pharmacol. *135*: 1828–1836.

Annamneedi, A., Gora, C., Dudas, A., Leray, X., Bozon, V., Crépieux, P., et al. (2023). Towards the convergent therapeutic potential of G protein-coupled receptors in autism spectrum disorders. Br. J. Pharmacol. bph.16216.

Bernaerts, S., Boets, B., Bosmans, G., Steyaert, J., and Alaerts, K. (2020). Behavioral effects of multiple-dose oxytocin treatment in autism: a randomized, placebo-controlled trial with long-term follow-up. Mol. Autism *11*: 6.

Birnbaumer, M. (2000). Vasopressin receptors. Trends Endocrinol. Metab. TEM *11*: 406–410.

Bolognani, F., Del Valle Rubido, M., Squassante, L., Wandel, C., Derks, M., Murtagh, L., et al. (2019). A phase 2 clinical trial of a vasopressin V1a receptor antagonist shows improved adaptive behaviors in men with autism spectrum disorder. Sci. Transl. Med. *11*: eaat7838.

Busnelli, M., Bulgheroni, E., Manning, M., Kleinau, G., and Chini, B. (2013). Selective and potent agonists and antagonists for investigating the role of mouse oxytocin receptors. J. Pharmacol. Exp. Ther. *346*: 318–327.

Busnelli, M., Saulière, A., Manning, M., Bouvier, M., Galés, C., and Chini, B. (2012). Functional selective oxytocin-derived agonists discriminate between individual G protein family subtypes. J. Biol. Chem. *287*: 3617–3629.

Camps, M., Hou, C., Sidiropoulos, D., Stock, J.B., Jakobs, K.H., and Gierschik, P. (1992). Stimulation of phospholipase C by guanine-nucleotide-binding protein beta gamma subunits. Eur. J. Biochem. *206*: 821–831.

Chaumont, F. de, Ey, E., Torquet, N., Lagache, T., Dallongeville, S., Imbert, A., et al. (2019). Real-time analysis of the behaviour of groups of mice via a depth-sensing camera and machine learning. Nat. Biomed. Eng. *3*: 930–942.

Daniels, N., Moerkerke, M., Steyaert, J., Bamps, A., Debbaut, E., Prinsen, J., et al. (2023). Effects of multiple-dose intranasal oxytocin administration on social responsiveness in children with autism: a randomized, placebo-controlled trial. Mol. Autism *14*: 16.

De Rubeis, S., He, X., Goldberg, A.P., Poultney, C.S., Samocha, K., Cicek, A.E., et al. (2014). Synaptic, transcriptional and chromatin genes disrupted in autism. Nature *515*: 209–215.

Dong, R., Goodbrake, C., Harrington, H.A., and Pogudin, G. (2023). Differential Elimination for Dynamical Models via Projections with Applications to Structural Identifiability. SIAM J. Appl. Algebra Geom. *7*: 194–235.

Drobac, E., Tricoire, L., Chaffotte, A.-F., Guiot, E., and Lambolez, B. (2010). Calcium imaging in single neurons from brain slices using bioluminescent reporters. J. Neurosci. Res. *88*: 695–711.

Elands, J., Barberis, C., and Jard, S. (1988). [3H]-[Thr4,Gly7]OT: a highly selective ligand for central and peripheral OT receptors. Am. J. Physiol. *254*: E31-38.

748 Ford, C.L., and Young, L.J. (2022). Refining oxytocin therapy for autism: context is key. Nat.
749 Rev. Neurol. *18*: 67–68.
750 Fröhlich, F., Weindl, D., Schälte, Y., Pathirana, D., Paszkowski, Ł., Lines, G.T., et al. (2021).
751 AMICI: high-performance sensitivity analysis for large ordinary differential equation models.
752 Bioinforma. Oxf. Engl. *37*: 3676–3677.
753 Goodwin, T.M., Paul, R., Silver, H., Spellacy, W., Parsons, M., Chez, R., et al. (1994). The
754 effect of the oxytocin antagonist atosiban on preterm uterine activity in the human. Am. J.
755 Obstet. Gynecol. *170*: 474–478.
756 Gora, C., Dudas, A., Vaugrente, O., Drobecq, L., Pecnard, E., Lefort, G., et al. (2024).
757 Deciphering autism heterogeneity: a molecular stratification approach in four mouse models.
758 Transl. Psychiatry *14*: 416.
759 Grimwood, S., and Hartig, P.R. (2009). Target site occupancy: emerging generalizations
760 from clinical and preclinical studies. Pharmacol. Ther. *122*: 281–301.
761 Guastella, A.J., Boulton, K.A., Whitehouse, A.J.O., Song, Y.J., Thapa, R., Gregory, S.G., et al.
762 (2023). The effect of oxytocin nasal spray on social interaction in young children with autism:
763 a randomized clinical trial. Mol. Psychiatry *28*: 834–842.
764 Guastella, A.J., Einfeld, S.L., Gray, K.M., Rinehart, N.J., Tonge, B.J., Lambert, T.J., et al.
765 (2010). Intranasal oxytocin improves emotion recognition for youth with autism spectrum
766 disorders. Biol. Psychiatry *67*: 692–694.
767 Haider, R.S., Matthees, E.S.F., Drube, J., Reichel, M., Zabel, U., Inoue, A., et al. (2022). β-
768 arrestin1 and 2 exhibit distinct phosphorylation-dependent conformations when coupling to
769 the same GPCR in living cells. Nat. Commun. *13*: 5638.
770 Hauser, A.S., Attwood, M.M., Rask-Andersen, M., Schiöth, H.B., and Gloriam, D.E. (2017).
771 Trends in GPCR drug discovery: new agents, targets and indications. Nat. Rev. Drug Discov.
772 *16*: 829–842.
773 Heydenreich, F.M., Plouffe, B., Rizk, A., Milić, D., Zhou, J., Breton, B., et al. (2022).
774 Michaelis-Menten Quantification of Ligand Signaling Bias Applied to the Promiscuous
775 Vasopressin V2 Receptor. Mol. Pharmacol. *102*: 139–149.
776 Hoare, S.R.J., Tewson, P.H., Quinn, A.M., Hughes, T.E., and Bridge, L.J. (2020). Analyzing
777 kinetic signaling data for G-protein-coupled receptors. Sci. Rep. *10*: 12263.
778 Hollander, E., Jacob, S., Jou, R., McNamara, N., Sikich, L., Tobe, R., et al. (2022). Balovaptan
779 vs Placebo for Social Communication in Childhood Autism Spectrum Disorder: A Randomized
780 Clinical Trial. JAMA Psychiatry *79*: 760–769.
781 Jacob, S., Veenstra-VanderWeele, J., Murphy, D., McCracken, J., Smith, J., Sanders, K., et
782 al. (2022). Efficacy and safety of balovaptan for socialisation and communication difficulties
783 in autistic adults in North America and Europe: a phase 3, randomised, placebo-controlled
784 trial. Lancet Psychiatry *9*: 199–210.
785 Janz, P., Knoflach, F., Bleicher, K., Belli, S., Biemans, B., Schnider, P., et al. (2023). Selective
786 oxytocin receptor activation prevents prefrontal circuit dysfunction and social behavioral
787 alterations in response to chronic prefrontal cortex activation in male rats. Front. Cell.
788 Neurosci. *17*: 1286552.
789 Jiang, L.I., Collins, J., Davis, R., Lin, K.-M., DeCamp, D., Roach, T., et al. (2007). Use of a cAMP
790 BRET sensor to characterize a novel regulation of cAMP by the sphingosine 1-phosphate/G13
791 pathway. J. Biol. Chem. *282*: 10576–10584.
792 Kamal, M., Marquez, M., Vauthier, V., Leloire, A., Froguel, P., Jockers, R., et al. (2009).
793 Improved donor/acceptor BRET couples for monitoring beta-arrestin recruitment to G
794 protein-coupled receptors. Biotechnol. J. *4*: 1337–1344.

Kat, R., Arroyo-Araujo, M., Vries, R.B.M. de, Koopmans, M.A., Boer, S.F. de, and Kas, M.J.H. (2022). Translational validity and methodological underreporting in animal research: A systematic review and meta-analysis of the Fragile X syndrome (Fmr1 KO) rodent model. Neurosci. Biobehav. Rev. *139*: 104722.

Kato, Y., Igarashi, N., Hirasawa, A., Tsujimoto, G., and Kobayashi, M. (1995). Distribution and developmental changes in vasopressin V2 receptor mRNA in rat brain. Differ. Res. Biol. Divers. *59*: 163–169.

Kenakin, T., Watson, C., Muniz-Medina, V., Christopoulos, A., and Novick, S. (2012). A simple method for quantifying functional selectivity and agonist bias. ACS Chem. Neurosci. *3*: 193–203.

Kilkenny, C., Browne, W.J., Cuthill, I.C., Emerson, M., and Altman, D.G. (2010). Improving bioscience research reporting: the ARRIVE guidelines for reporting animal research. PLoS Biol. *8*: e1000412.

Koehbach, J., O'Brien, M., Muttenthaler, M., Miazzo, M., Akcan, M., Elliott, A.G., et al. (2013). Oxytocic plant cyclotides as templates for peptide G protein-coupled receptor ligand design. Proc. Natl. Acad. Sci. U. S. A. *110*: 21183–21188.

Kolb, P., Kenakin, T., Alexander, S.P.H., Bermudez, M., Bohn, L.M., Breinholt, C.S., et al. (2022). Community guidelines for GPCR ligand bias: IUPHAR review 32. Br. J. Pharmacol. *179*: 3651–3674.

Lee, J., Kwag, R., Lee, S., Kim, D., Woo, J., Cho, Y., et al. (2021). Discovery of G Protein-Biased Ligands against 5-HT7R. J. Med. Chem. *64*: 7453–7467.

Lee, S.A., Eyeson, R., Cheever, M.L., Geng, J., Verkhusha, V.V., Burd, C., et al. (2005). Targeting of the FYVE domain to endosomal membranes is regulated by a histidine switch. Proc. Natl. Acad. Sci. U. S. A. *102*: 13052–13057.

Leng, G., Leng, R.I., and Ludwig, M. (2022). Oxytocin-a social peptide? Deconstructing the evidence. Philos. Trans. R. Soc. Lond. B. Biol. Sci. *377*: 20210055.

Lewis, E.M., Stein-O'Brien, G.L., Patino, A.V., Nardou, R., Grossman, C.D., Brown, M., et al. (2020). Parallel Social Information Processing Circuits Are Differentially Impacted in Autism. Neuron *108*: 659-675.e6.

Lindenmaier, Z., Ellegood, J., Stuive, M., Easson, K., Yee, Y., Fernandes, D., et al. (2022). Examining the effect of chronic intranasal oxytocin administration on the neuroanatomy and behavior of three autism-related mouse models. NeuroImage *257*: 119243.

Marir, R., Virsolvy, A., Wisniewski, K., Mion, J., Haddou, D., Galibert, E., et al. (2013). Pharmacological characterization of FE 201874, the first selective high affinity rat V1A vasopressin receptor agonist. Br. J. Pharmacol. *170*: 278–292.

Mientjes, E.J., Nieuwenhuizen, I., Kirkpatrick, L., Zu, T., Hoogeveen-Westerveld, M., Severijnen, L., et al. (2006). The generation of a conditional Fmr1 knock out mouse model to study Fmrp function in vivo. Neurobiol. Dis. *21*: 549–555.

Namkung, Y., Le Gouill, C., Lukashova, V., Kobayashi, H., Hogue, M., Khoury, E., et al. (2016). Monitoring G protein-coupled receptor and β-arrestin trafficking in live cells using enhanced bystander BRET. Nat. Commun. *7*: 12178.

Nehmé, R., Carpenter, B., Singhal, A., Strege, A., Edwards, P.C., White, C.F., et al. (2017). Mini-G proteins: Novel tools for studying GPCRs in their active conformation. PloS One *12*: e0175642.

Ostrowski, N.L., Lolait, S.J., Bradley, D.J., O'Carroll, A.M., Brownstein, M.J., and Young, W.S. (1992). Distribution of V1a and V2 vasopressin receptor messenger ribonucleic acids in rat liver, kidney, pituitary and brain. Endocrinology *131*: 533–535.

Pan, L., Zheng, L., Wu, X., Zhu, Z., Wang, S., Lu, Y., et al. (2022). A short period of early life oxytocin treatment rescues social behavior dysfunction via suppression of hippocampal hyperactivity in male mice. Mol. Psychiatry *27*: 4157–4171.

Pantouli, F., Pujol, C.N., Derieux, C., Fonteneau, M., Pellissier, L.P., Marsol, C., et al. (2024). Acute, chronic and conditioned effects of intranasal oxytocin in the mu-opioid receptor knockout mouse model of autism: Social context matters. Neuropsychopharmacol. Off. Publ. Am. Coll. Neuropsychopharmacol.

Park, S.M., Chen, M., Schmerberg, C.M., Dulman, R.S., Rodriguiz, R.M., Caron, M.G., et al. (2016). Effects of β-Arrestin-Biased Dopamine D2 Receptor Ligands on Schizophrenia-Like Behavior in Hypoglutamatergic Mice. Neuropsychopharmacol. Off. Publ. Am. Coll. Neuropsychopharmacol. *41*: 704–715.

Parker, K.J., Oztan, O., Libove, R.A., Mohsin, N., Karhson, D.S., Sumiyoshi, R.D., et al. (2019). A randomized placebo-controlled pilot trial shows that intranasal vasopressin improves social deficits in children with autism. Sci. Transl. Med. *11*: eaau7356.

Parker, K.J., Oztan, O., Libove, R.A., Sumiyoshi, R.D., Jackson, L.P., Karhson, D.S., et al. (2017). Intranasal oxytocin treatment for social deficits and biomarkers of response in children with autism. Proc. Natl. Acad. Sci. U. S. A. *114*: 8119–8124.

Passoni, I., Leonzino, M., Gigliucci, V., Chini, B., and Busnelli, M. (2016). Carbetocin is a Functional Selective Gq Agonist That Does Not Promote Oxytocin Receptor Recycling After Inducing β-Arrestin-Independent Internalisation. J. Neuroendocrinol. *28*: n/a.

Peñagarikano, O., Lázaro, M.T., Lu, X.-H., Gordon, A., Dong, H., Lam, H.A., et al. (2015). Exogenous and evoked oxytocin restores social behavior in the Cntnap2 mouse model of autism. Sci. Transl. Med. *7*: 271ra8.

Pieretti, M., Zhang, F.P., Fu, Y.H., Warren, S.T., Oostra, B.A., Caskey, C.T., et al. (1991). Absence of expression of the FMR-1 gene in fragile X syndrome. Cell *66*: 817–822.

Pintacuda, G., Hsu, Y.-H.H., Tsafou, K., Li, K.W., Martín, J.M., Riseman, J., et al. (2023). Protein interaction studies in human induced neurons indicate convergent biology underlying autism spectrum disorders. Cell Genomics 100250.

Quintana, D.S., Rokicki, J., Meer, D. van der, Alnæs, D., Kaufmann, T., Córdova-Palomera, A., et al. (2019). Oxytocin pathway gene networks in the human brain. Nat. Commun. *10*: 668.

Raue, A., Schilling, M., Bachmann, J., Matteson, A., Schelker, M., Kaschek, D., et al. (2013). Lessons learned from quantitative dynamical modeling in systems biology. PloS One *8*: e74335.

Rigney, N., Vries, G.J. de, Petrulis, A., and Young, L.J. (2022). Oxytocin, Vasopressin, and Social Behavior: From Neural Circuits to Clinical Opportunities. Endocrinology *163*: bqac111.

Satterstrom, F.K., Kosmicki, J.A., Wang, J., Breen, M.S., De Rubeis, S., An, J.-Y., et al. (2020). Large-Scale Exome Sequencing Study Implicates Both Developmental and Functional Changes in the Neurobiology of Autism. Cell *180*: 568-584.e23.

Schälte, Y., Fröhlich, F., Jost, P.J., Vanhoefer, J., Pathirana, D., Stapor, P., et al. (2023). pyPESTO: a modular and scalable tool for parameter estimation for dynamic models. Bioinforma. Oxf. Engl. *39*: btad711.

Schmiester, L., Schälte, Y., Bergmann, F.T., Camba, T., Dudkin, E., Egert, J., et al. (2021). PEtab-Interoperable specification of parameter estimation problems in systems biology. PLoS Comput. Biol. *17*: e1008646.

Schnider, P., Bissantz, C., Bruns, A., Dolente, C., Goetschi, E., Jakob-Roetne, R., et al. (2020). Discovery of Balovaptan, a Vasopressin 1a Receptor Antagonist for the Treatment of Autism Spectrum Disorder. J. Med. Chem. *63*: 1511–1525.

Stevenson, E.L., and Caldwell, H.K. (2012). The vasopressin 1b receptor and the neural regulation of social behavior. Horm. Behav. *61*: 277–282.

Strakova, Z., Copland, J.A., Lolait, S.J., and Soloff, M.S. (1998). ERK2 mediates oxytocin-stimulated PGE2 synthesis. Am. J. Physiol. *274*: E634-641.

Strakova, Z., and Soloff, M.S. (1997). Coupling of oxytocin receptor to G proteins in rat myometrium during labor: Gi receptor interaction. Am. J. Physiol. *272*: E870-876.

Terrillon, S., Durroux, T., Mouillac, B., Breit, A., Ayoub, M.A., Taulan, M., et al. (2003). Oxytocin and vasopressin V1a and V2 receptors form constitutive homo- and heterodimers during biosynthesis. Mol. Endocrinol. Baltim. Md *17*: 677–691.

Theofanopoulou, C., Andirkó, A., Boeckx, C., and Jarvis, E.D. (2022). Oxytocin and vasotocin receptor variation and the evolution of human prosociality. Compr. Psychoneuroendocrinology *11*: 100139.

Umbricht, D., Del Valle Rubido, M., Hollander, E., McCracken, J.T., Shic, F., Scahill, L., et al. (2017). A Single Dose, Randomized, Controlled Proof-Of-Mechanism Study of a Novel Vasopressin 1a Receptor Antagonist (RG7713) in High-Functioning Adults with Autism Spectrum Disorder. Neuropsychopharmacol. Off. Publ. Am. Coll. Neuropsychopharmacol. *42*: 1914–1923.

Valstad, M., Alvares, G.A., Egknud, M., Matziorinis, A.M., Andreassen, O.A., Westlye, L.T., et al. (2017). The correlation between central and peripheral oxytocin concentrations: A systematic review and meta-analysis. Neurosci. Biobehav. Rev. *78*: 117–124.

Verheij, C., Bakker, C.E., Graaff, E. de, Keulemans, J., Willemsen, R., Verkerk, A.J., et al. (1993). Characterization and localization of the FMR-1 gene product associated with fragile X syndrome. Nature *363*: 722–724.

Wan, Q., Okashah, N., Inoue, A., Nehmé, R., Carpenter, B., Tate, C.G., et al. (2018). Mini G protein probes for active G protein-coupled receptors (GPCRs) in live cells. J. Biol. Chem. *293*: 7466–7473.

Williams, P.D., Clineschmidt, B.V., Erb, J.M., Freidinger, R.M., Guidotti, M.T., Lis, E.V., et al. (1995). 1-(1-[4-[(N-acetyl-4-piperidinyl)oxy]-2-methoxybenzoyl]piperidin-4- yl)-4H-3,1-benzoxazin-2(1H)-one (L-371,257): a new, orally bioavailable, non-peptide oxytocin antagonist. J. Med. Chem. *38*: 4634–4636.

Young, W.S., Li, J., Wersinger, S.R., and Palkovits, M. (2006). The vasopressin 1b receptor is prominent in the hippocampal area CA2 where it is unaffected by restraint stress or adrenalectomy. Neuroscience *143*: 1031–1039.

FIGURE LEGENDS

Figure 1 Pharmacological systemic analysis of OT and AVP effects on murine oxytocin and vasopressin receptors in Neuro-2a cells

(**A**) schematic representation on miniGq, miniGi, miniGs, β-arrestin-1, β-arrestin-2 recruitments, intracellular Ca^{2+} mobilisation, cAMP production or forskolin-induced inhibition, and membrane CAAX and endosome FYVE internalisation of mouse OTR, V_{1A}, V_{1B}, V_2 receptors following OT (red) and AVP (blue) stimulation in the murine Neuro-2a cell line. (**B**) Mathematical model equation fitting with β-arrestin-2 recruitment, internalisation and recycling profiles of the four receptors. (**C**) Spider plots illustrate the relative effect of OT and AVP on the ten intracellular inputs of these four receptors. (**D**) Radar plot summarise the robust predicted affinity (K_D) and kinetic parameters of β-arrestin-2 recruitment (k_τ), internalisation (k_{int}) and recycling (k_{rec}) for each receptor and endogenous ligand, except for OT on the V_{1A} receptor and AVP on OTR. A, agonist; AVP, arginine vasopressin; ext, extracellular space; int, intracellular compartment; OT, oxytocin; R, receptor; RAB, receptor-agonist-β-arrestin-2 complex; RI, internalised receptor.

Figure 2 Effect of orthologs and synthetic ligands on murine oxytocin and vasopressin receptors in Neuro-2a cells

(**A**) Bias plot of an equimolar comparison of the orthologs isotocin (slate), mesotocin (khaki), and vasotocin (mauve) in miniGq and β-arrestin-2 recruitment at mouse OTR, V_{1A}, V_{1B}, V_2 receptors in the murine Neuro-2a cell line, with OT (red) and AVP (blue) as reference ligands for OTR and vasopressin receptors, respectively. (**B**) Bias plot of the synthetic ligands TGOT (mustard), RO6958375 (purple), carbetocin (light blue) and kB7 (light brown) in miniGq and β-arrestin-2 recruitment at the four receptors. (**C**) Dose-response curves of the OTR agonists

947 TGOT and RO6958375 in miniGq and β-arrestin-2 recruitment at the four receptors. (**D**) Dose-
948 response curves of the antagonists atosiban (yellow), RO6893074 (green) and L-371,257 (dark
949 brown) in the presence of OT and AVP at their EC_{80} concentrations on OTR and vasopressin
950 receptor miniGq and β-arrestin-2 recruitment. AVP, arginine vasopressin; OT, oxytocin.
951
952 **Figure 3 Acute and subchronic effect of OT and AVP on social motivation and exploration in**
953 ***Fmr1* KO and WT mice**
954 In the Live Mouse Tracker, the cumulative time in nose contact, social approach and huddling
955 behaviours over a 10 min period were compared following 15 minutes of acute (**A**) or
956 subchronic (**B**) intranasal administration of OT or AVP at low and moderate dose in WT (NaCl
957 0.9% (SAL; grey): n = 34, 10 males and 24 females; OT 20 $\mu g.kg^{-1}$ (pink): n = 14, 4 males and
958 10 females; OT 40 $\mu g.kg^{-1}$ (red): n = 8, 4 males and 4 females; AVP 20 $\mu g.kg^{-1}$ (light blue): n =
959 9, 5 males and 4 females; AVP 40 $\mu g.kg^{-1}$ (dark blue): n = 8, 4 males and 4 females) and *Fmr1*
960 KO mice (SAL (grey): n = 46, 22 males and 24 females; OT 20 $\mu g.kg^{-1}$ (pink): n = 8, 4 males and
961 4 females; OT 40 $\mu g.kg^{-1}$ (red): n = 8, 4 males and 4 females; AVP 20 $\mu g.kg^{-1}$ (light blue): n =
962 16, 5 males and 11 females; AVP 40 $\mu g.kg^{-1}$ (dark blue): n = 12, 8 males and 4 females). Data
963 are presented as mean ± sd (raw values, mean and statistics in Table S5). Statistical analysis
964 was conducted using Kruskal-Wallis tests followed by Dunn post hoc tests with asterisks

indicating treatment effect (p = P adjusted): *p<0.05, **p<0.01, ***p<0.001, ****p<0.0001. AVP, arginine vasopressin; KO, *Fmr1* KO mice; OT, oxytocin; SAL, saline; WT, wild-type.

Figure 4 Acute and subchronic effect of TGOT, RO6958375 and RO6893074 on social motivation and exploration in *Fmr1* KO and WT mice

In the Live Mouse Tracker, the cumulative time in nose contact, social approach and huddling behaviours over a 10 min period were compared following 15 minutes of acute (**A**) or subchronic (**B**) administration of TGOT (intranasal) and RO6958375 (subcutaneous) OTR agonists and RO6893074 V_{1A} antagonist (intraperitoneal) at low, moderate and high dose in WT (SAL for TGOT (grey): n = 34, 10 males and 24 females; TGOT 20 µg.kg^{-1} (light brown): n = 10, 4 males and 6 females; TGOT 40 µg.kg^{-1} (brown): n = 10, 6 males and 4 females; PBS 1X for RO6958375 (PBS; grey): n = 19, 10 males and 9 females; RO6958375 0.03 mg.kg^{-1} (light violet): n = 9, 5 males and 4 females; RO6958375 0.06 mg.kg^{-1} (violet): n = 8, 4 males and 4 females; RO6958375 0.12 mg.kg^{-1} (dark violet): n = 10, 5 males and 5 females; 0.1% Tween-80 for RO6893074 (VEH; grey): n = 20, 10 males and 10 females; RO6893074 25 mg.kg^{-1} (light green): n = 11, 5 males and 6 females; RO6893074 50 mg.kg^{-1} (green): n = 8, 4 males and 4 females; RO6893074 100 mg.kg^{-1} (dark green): n = 10, 4 males and 6 females) and *Fmr1* KO mice (0 = NaCl 0.9% for TGOT (grey): n = 46, 22 males and 24 females; TGOT 20 µg.kg^{-1} (light brown): n = 12, 6 males and 6 females; TGOT 40 µg.kg^{-1} (brown): n = 13, 7 males and 6 females; 0 = PBS 1X for RO6958375 (grey): n = 27, 11 males and 16 females; RO6958375 0.03 mg.kg^{-1} (light violet): n = 13, 4 males and 9 females; RO6958375 0.06 mg.kg^{-1} (violet): n = 14, 5 males and 9 females; RO6958375 0.12 mg.kg^{-1} (dark violet): n = 12, 6 males and 6 females; 0 = 0.1% Tween-80 for RO6893074 (grey): n = 21, 11 males and 10 females; RO6893074 25 mg.kg^{-1} (light green): n = 9, 4 males and 5 females; RO6893074 50 mg.kg^{-1} (green): n = 14, 6 males

989 and 8 females; RO6893074 100 mg.kg^{-1} (dark green): n = 10, 4 males and 6 females). Data are
990 presented as mean ± sd (raw values, mean and statistics in Table S5). Statistical analysis was
991 conducted using Kruskal-Wallis tests followed by Dunn post hoc tests with asterisks indicating
992 treatment effect (*p* = P adjusted): *p<0.05, **p<0.01, ***p<0.001, ****p<0.0001. KO, *Fmr1*
993 KO mice; OTR, oxytocin receptor; PBS, Phosphate-buffered saline; SAL, saline; TGOT,
994 (Thr^4,Gly^7)-oxytocin; VEH; vehicle; WT, wild-type.
995

Figure 1 Pharmacological systemic analysis of OT and AVP effects on murine oxytocin and vasopressin receptors in Neuro-2a cells

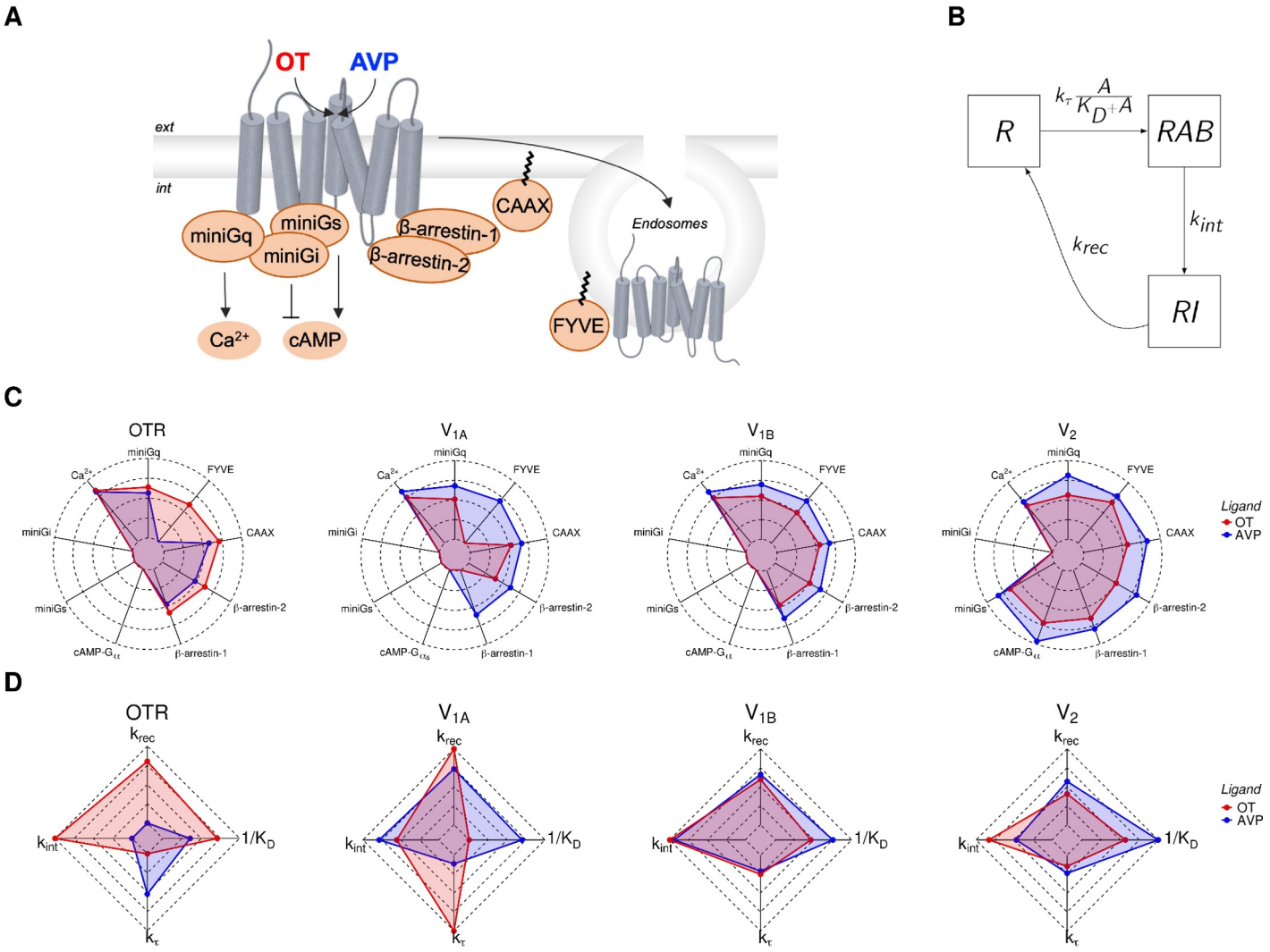

Figure 2 Effect of orthologs and synthetic ligands on murine oxytocin and vasopressin receptors in Neuro-2a cells

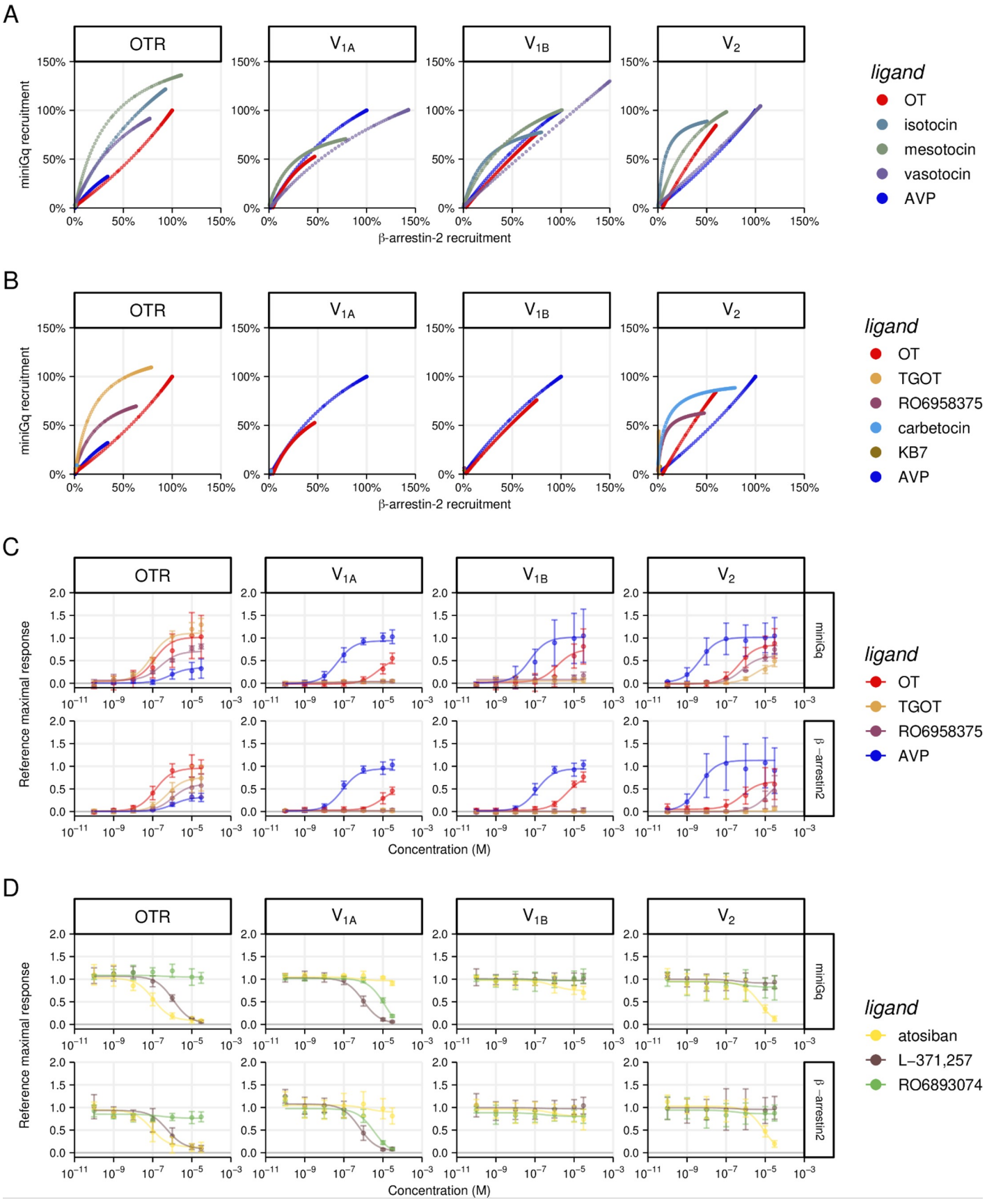

Figure 3 Acute and subchronic effect of OT and AVP on social motivation and exploration in *Fmr1* KO and WT mice

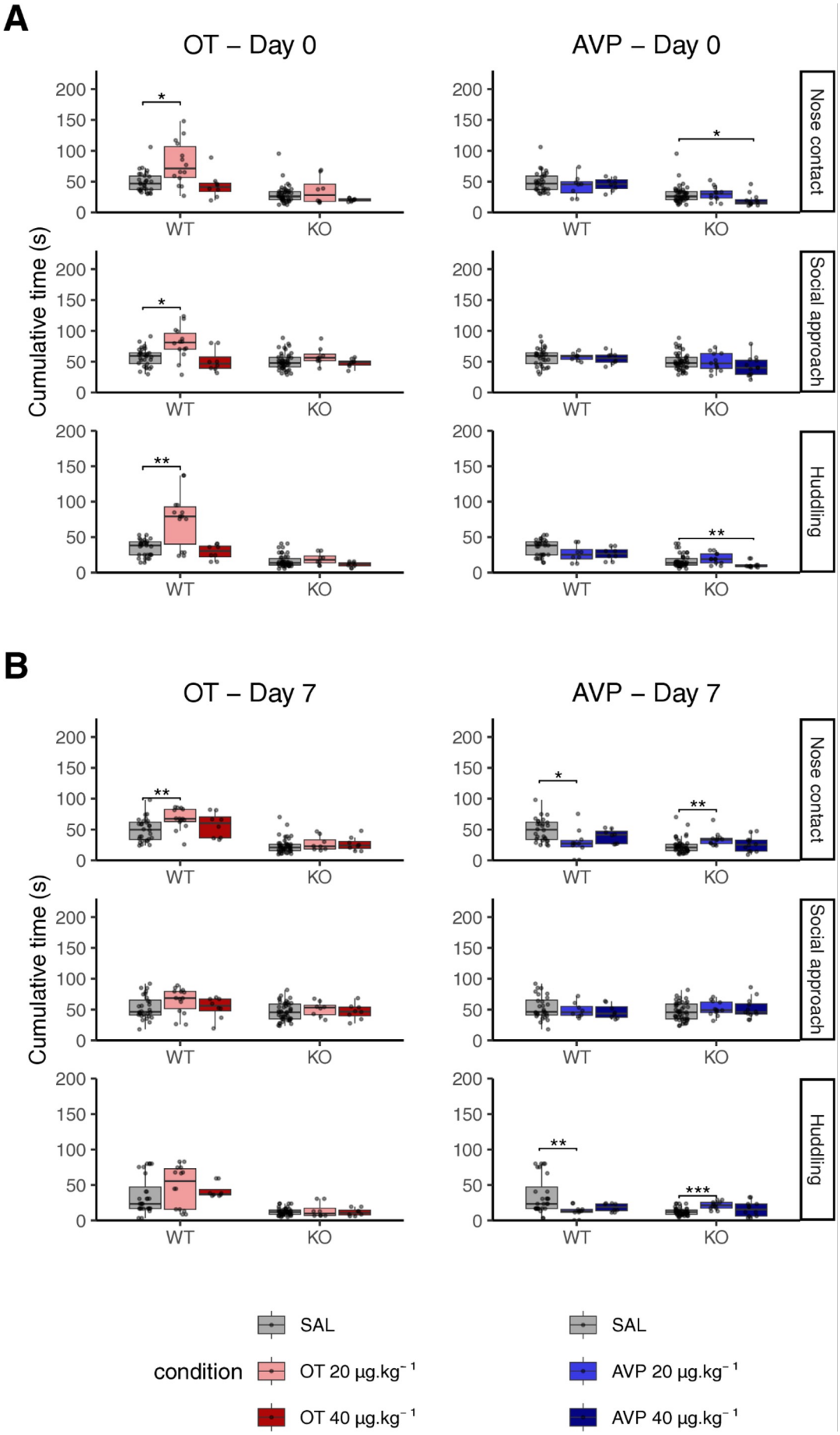

Figure 4 Acute and subchronic effect of TGOT, RO6958375 and RO6893074 on social motivation and exploration in *Fmr1* KO and WT mice

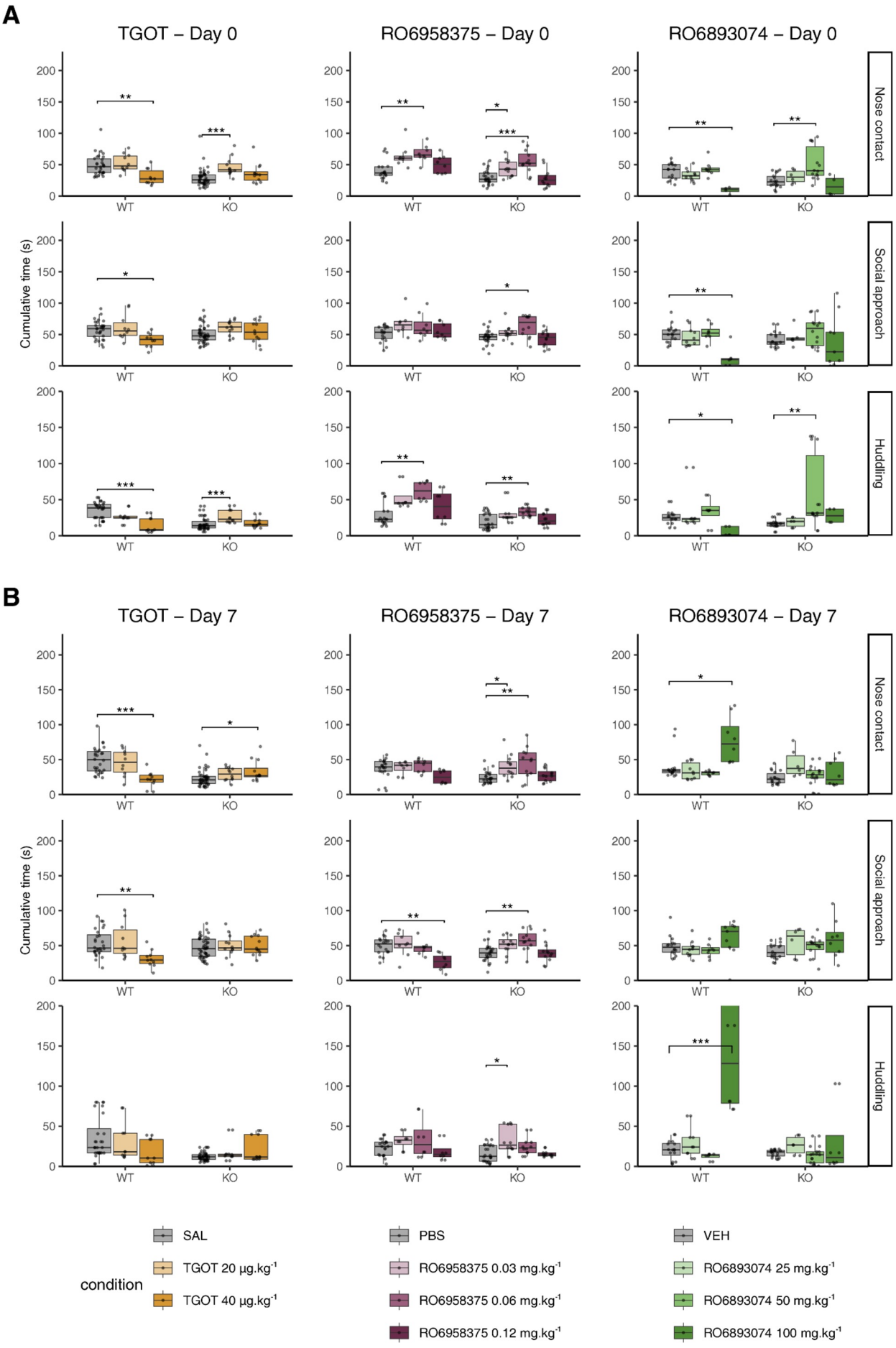

996 **TABLE LEGENDS**

997

998 **Table 1: Bias factors of the ligands on murine oxytocin and vasopressin receptors in Neuro-**

999 **2a**

1000 Statistical analysis was conducted using Student t-test with asterisks indicating bias effect (p

1001 = P value): *p<0.05, **p<0.01, ***p<0.001, ****p<0.0001. RE, relative efficiency compared

1002 to the reference ligand 10Δlog(τ/Ka); bias factor, REβarr2/REGq; §, ligand of reference.

Receptor	Ligand	log(τ/Ka)		Δlog(τ/Ka)			ΔΔlog(τ/Ka)	*RE*		*Bias factor*
		Gq	βarr2	Gq	βarr2			Gq	βarr2	
OTR	OT§	6.68 ± 0.06	6.82 ± 0.07	0.00 ± 0.08	0.00 ± 0.09		0.00 ± 0.13	1.00	1.00	1
OTR	TGOT	7.00 ± 0.08	6.07 ± 0.04	0.32 ± 0.10	-0.75 ± 0.08	***	-1.13 ± 0.14	02.09	0.18	0.08
OTR	RO6958375	6.39 ± 0.07	5.70 ± 0.05	-0.30 ± 0.09	-1.12 ± 0.08	***	-0.89 ± 0.13	0.51	0.08	0.15
OTR	isotocin	6.31 ± 0.03	5.96 ± 0.05	-0.37 ± 0.07	-0.86 ± 0.08	***	-0.50 ± 0.12	0.43	0.14	0.32
OTR	mesotocin	7.35 ± 0.05	6.75 ± 0.04	0.67 ± 0.07	-0.07 ± 0.08	****	-0.76 ± 0.12	4.69	0.85	0.18
OTR	vasotocin	7.18 ± 0.10	6.66 ± 0.04	0.49 ± 0.11	-0.16 ± 0.08	*	-0.70 ± 0.18	3.11	0.69	0.22
OTR	carbetocin	ND	ND	ND	ND		-0.13 ± 0.85	ND	ND	ND
OTR	KB7	ND	ND	ND	ND		-0.12 ± 1.18	ND	ND	ND
OTR	AVP	5.63 ± 0.11	5.44 ± 0.09	-1.05 ± 0.12	-1.38 ± 0.12	*	-0.31 ± 0.15	0.09	0.04	0.47
V1A	OT	4.80 ± 0.11	4.63 ± 0.10	-2.42 ± 0.12	-2.43 ± 0.11		0.02 ± 0.17	0.00	0.00	0.98
V1A	TGOT	ND	ND	ND	ND		0.15 ± 0.90	ND	ND	ND
V1A	RO6958375	5.74 ± 0.49	ND	-1.49 ± 0.50	ND		0.47 ± 0.85	0.03	ND	ND
V1A	isotocin	ND	ND	ND	ND		0.15 ± 1.03	ND	ND	ND
V1A	mesotocin	5.28 ± 0.06	4.89 ± 0.05	-1.95 ± 0.08	-2.17 ± 0.06	*	-0.27 ± 0.14	0.01	0.01	0.6
V1A	vasotocin	7.24 ± 0.08	7.07 ± 0.04	0.01 ± 0.10	0.01 ± 0.06		0.00 ± 0.12	1.02	1.02	1
V1A	carbetocin	ND	ND	ND	ND		0.14 ± 1.16	ND	ND	ND
V1A	KB7	ND	ND	ND	ND		0.20 ± 0.82	ND	ND	ND
V1A	AVP§	7.23 ± 0.06	7.06 ± 0.04	0.00 ± 0.08	0.00 ± 0.06		0.00 ± 0.11	1.00	1.00	1
V1B	OT	5.25 ± 0.08	5.24 ± 0.04	-1.72 ± 0.10	-1.67 ± 0.06		0.11 ± 0.18	0.02	0.02	1.14
V1B	TGOT	ND	ND	ND	ND		0.12 ± 1.14	ND	ND	ND
V1B	RO6958375	ND	ND	ND	ND		0.10 ± 1.18	ND	ND	ND
V1B	isotocin	5.71 ± 0.08	5.03 ± 0.05	-1.26 ± 0.11	-1.88 ± 0.06	*	-0.59 ± 0.17	0.05	0.01	0.24
V1B	mesotocin	5.88 ± 0.10	5.42 ± 0.07	-1.09 ± 0.12	-1.49 ± 0.08		-0.41 ± 0.18	0.08	0.03	0.4
V1B	vasotocin	7.44 ± 0.07	7.39 ± 0.04	0.47 ± 0.10	0.49 ± 0.06		0.02 ± 0.15	2.95	03.07	01.04
V1B	carbetocin	ND	ND	ND	ND		0.21 ± 1.07	ND	ND	ND
V1B	KB7	ND	ND	ND	ND		0.10 ± 1.16	ND	ND	ND
V1B	AVP§	6.97 ± 0.07	6.91 ± 0.04	0.00 ± 0.10	0.00 ± 0.06		0.00 ± 0.18	1.00	1.00	1
V2	OT	6.18 ± 0.05	5.86 ± 0.06	-2.11 ± 0.14	-2.52 ± 0.15	*	-0.29 ± 0.19	0.01	0.00	0.39
V2	TGOT	5.06 ± 0.12	ND	-3.23 ± 0.18	ND		1.12 ± 0.72	0.00	ND	ND
V2	RO6958375	5.78 ± 0.14	4.60 ± 0.13	-2.51 ± 0.19	-3.78 ± 0.19	*	-1.24 ± 0.21	0.00	0.00	0.05
V2	isotocin	6.08 ± 0.06	4.99 ± 0.12	-2.21 ± 0.14	-3.39 ± 0.18	***	-1.19 ± 0.19	0.01	0.00	0.07
V2	mesotocin	6.70 ± 0.07	6.14 ± 0.03	-1.58 ± 0.15	-2.24 ± 0.14	**	-0.63 ± 0.17	0.03	0.01	0.22
V2	vasotocin	8.19 ± 0.16	8.29 ± 0.06	-0.10 ± 0.20	-0.09 ± 0.15		-0.02 ± 0.21	0.80	0.82	01.03
V2	carbetocin	6.00 ± 0.05	4.55 ± 0.09	-2.29 ± 0.14	-3.83 ± 0.16	**	-1.48 ± 0.19	0.01	0.00	0.03
V2	KB7	ND	ND	ND	ND		-0.07 ± 0.77	ND	ND	ND
V2	AVP§	8.29 ± 0.13	8.38 ± 0.14	0.00 ± 0.18	0.00 ± 0.19		0.00 ± 0.22	1.00	1.00	1

1003

1004

SUPPLEMENTARY INFORMATION

Table of contents

Supplementary Materials and Methods . . . 1
Supplementary Figures . . . 2
Figure S1: Relative efficacy and potency of OT and AVP on murine oxytocin and vasopressin receptors in Neuro-2a cells . . . 2
Figure S2: Relative efficacy and potency of OT and AVP on human oxytocin and vasopressin receptors in HEK293A cells . . . 3
Figure S3: Kinetic modelling of OT and AVP on murine oxytocin and vasopressin receptors in Neuro-2a cells . . . 3
Figure S4: Relative efficacy and potency of orthologs and synthetic ligands on murine oxytocin and vasopressin receptors in Neuro-2a cells . . . 4
Figure S5: F*mr1* KO males and females display social impairments compared to WT mice in the Live Mouse Tracker 5
Figure S6: Effect of OT and AVP on social motivation, isolation and anxious-like behaviours in *Fmr1* KO and WT mice 6
Figure S7: Effect of TGOT, RO6958375 and RO6893074 on social motivation, isolation and anxious-like behaviours in *Fmr1* KO and WT mice . . . 7

Supplementary Materials and Methods

Cell culture, G protein, beta-arrestin and internalisation assays using Bioluminescence Resonance Energy Transfer (BRET)
Human embryonic kidney 293A (HEK293A; ATCC, Manassas, VA, USA, CRL-1573™, RRID:CVCL_6910) cells were cultured in Dulbecco's Modified Eagle Medium (DMEM; CM1DME68-01, Eurobio, France) supplemented with 10% (v/v) foetal bovine serum (CVFSVF00-01, Eurobio, France) and 1% penicillin/streptomycin (100 $U.mL^{-1}$, 100 $\mu g.mL^{-1}$ respectively; 15140-122, Eurobio, France) and maintained at 37°C with 5% CO_2. When reaching 90% confluency, cells were washed with PBS 1X (CS1PBS01K-BP, Eurobio, France) followed by trypsin (0.5 $g.L^{-1}$, L-EDTA 0.2 $g.L^{-1}$, without phenol red; CEZTDA00-0U, Eurobio, France) treatment. After cell counting, cells were transiently transfected in suspension using the Metafectene Pro transfection reagent (T040-5.0, BioNTex Laboratories, Germany) according to the manufacturer's protocol.
In 96-well plates (30196, SPL Life Sciences, Korea), HEK293A cells (70, 000 cells/well) were transiently co-transfected with the human oxytocin receptor *OXTR* or human vasopressin receptors *AVPR1a, AVPR1b* subcloned with restriction enzymes HindIII and XhoI in pcDNA3 plasmid or with the *AVPR2* receptors in pcDNA3.1(+) plasmid, fused in their C-terminus to the BRET donor *Renilla reniformis* luciferase (RLuc8) at 25 ng per well, along with BRET acceptor sensors containing a yellow fluorescent proteins (YFP, Venus or YPET) at 50 ng per well each, miniGq or or YPET-β-arrestin-2. 48 hours after transfection, HEK293A cells were starved for 4 hours in phenol red-free DMEM (21063-029, Gibco, France) at 37°C in 5% CO_2. Cells incubated with cœlenterazine substrate (5 µM) were first measured for 5 minutes at 480 ± 20 nm and 530 ± 25 nm measurements (Mithras2 LB 943 with the Mikrowin 2010 software, Berthold Technologies GmbH & Co., Germany). Then, cells were rapidly stimulated with the different agonists at 3.10^{-5} M, 10^{-5} M, 10^{-6} M, 10^{-7} M, 10^{-8} M, 10^{-9} M, 10^{-10} M diluted in PBS 1X and HEPES 10 mM final, or PBS 1X and HEPES 10 mM alone for the baseline, then 96-well plates were recorded for 30 minutes.

Supplementary Figures

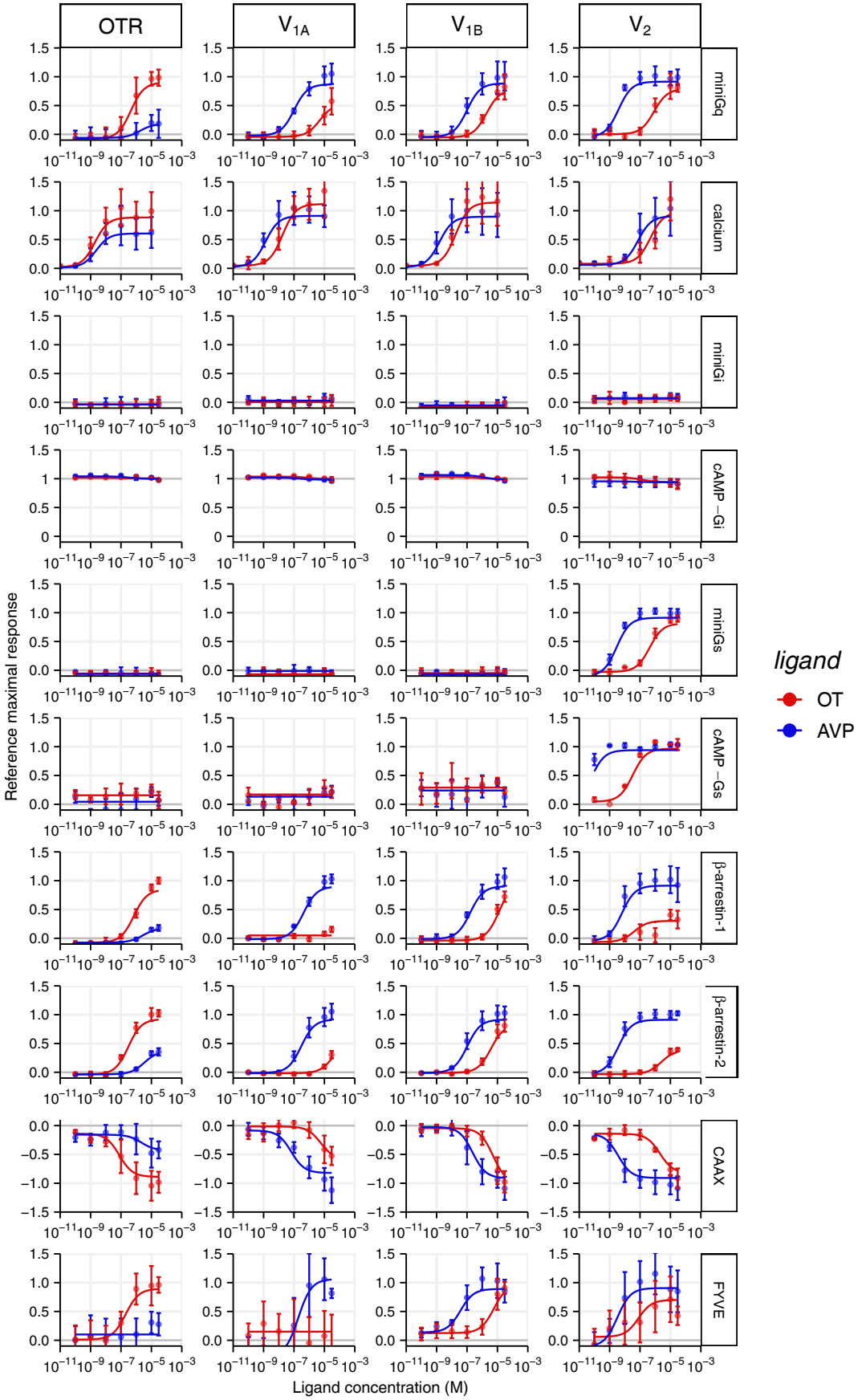

Figure S1: Relative efficacy and potency of OT and AVP on murine oxytocin and vasopressin receptors in Neuro-2a cells

Relative dose-response of OT (red) and AVP (blue) on miniGq, miniGi, miniGs, β-arrestin-1, β-arrestin-2 recruitment, intracellular Ca^{2+} mobilisation, cAMP production (cAMP - Gs) or forskoline-induced inhibition (cAMP - Gi), and CAAX and FYVE internalisation profiles of mouse OTR, V_{1A}, V_{1B}, V_2 receptors in murine Neuro-2A cell lines. The dose-response curve represents the mean of the biological replicates (n = 3-5 per sensor; Table S1).

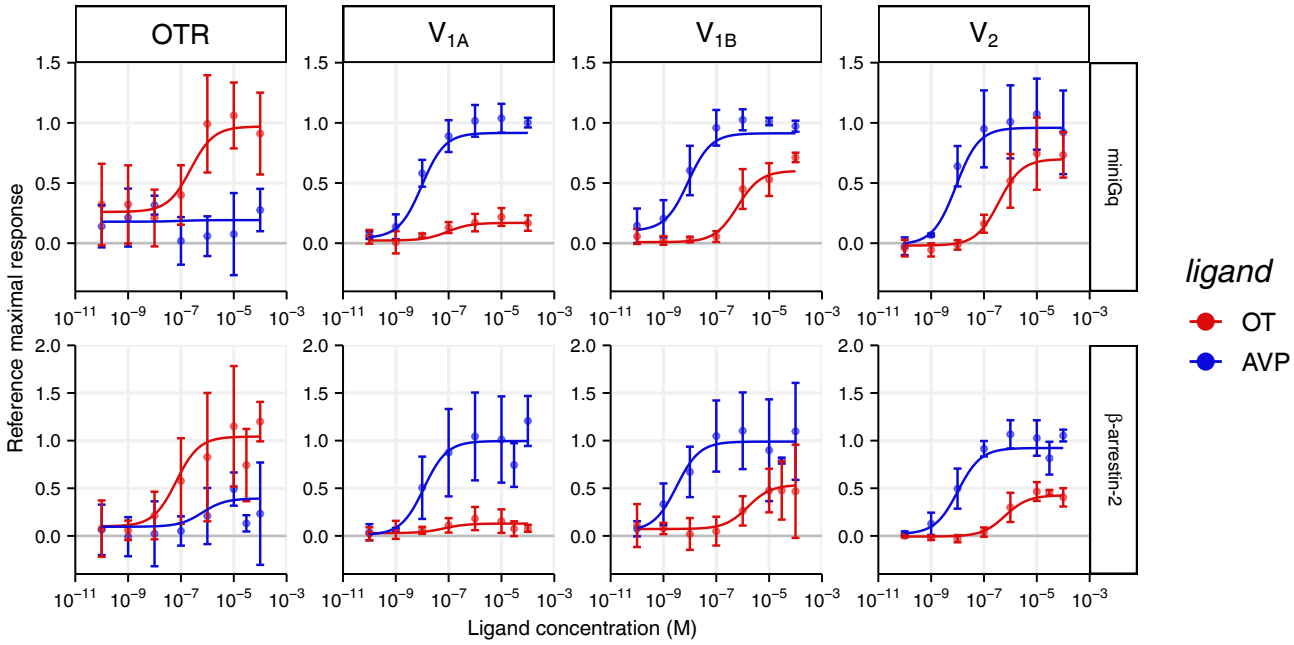

Figure S2: Relative efficacy and potency of OT and AVP on human oxytocin and vasopressin receptors in HEK293A cells

Relative dose-response of OT (red) and AVP (blue) on miniGq, and β-arrestin-2 recruitment profiles of human OTR, V_{1A}, V_{1B}, V_2 receptors in human HEK293A cell lines. The dose-response curve represents the mean of the biological replicates (n = 3-5 per sensor; Table S2).

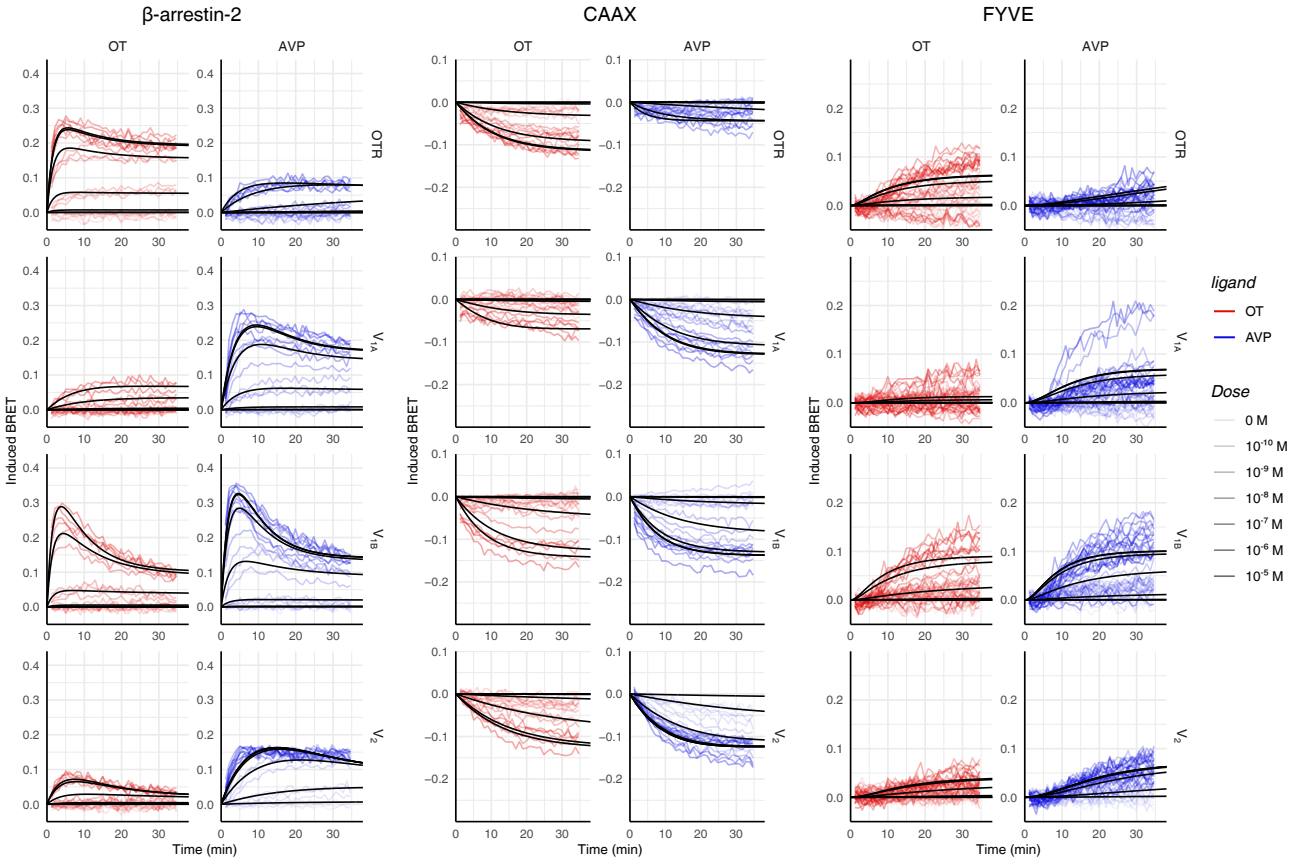

Figure S3: Kinetic modelling of OT and AVP on murine oxytocin and vasopressin receptors in Neuro-2a cells

Kinetics and model fitting of OT (red) and AVP (blue) as reference ligands on β-arrestin-2 recruitment, and CAAX and FYVE internalisation profiles of mouse OTR, V_{1A}, V_{1B}, V_2 receptors in murine Neuro-2A cell lines (n = 3-5 per sensor; Tables S1 and S3).

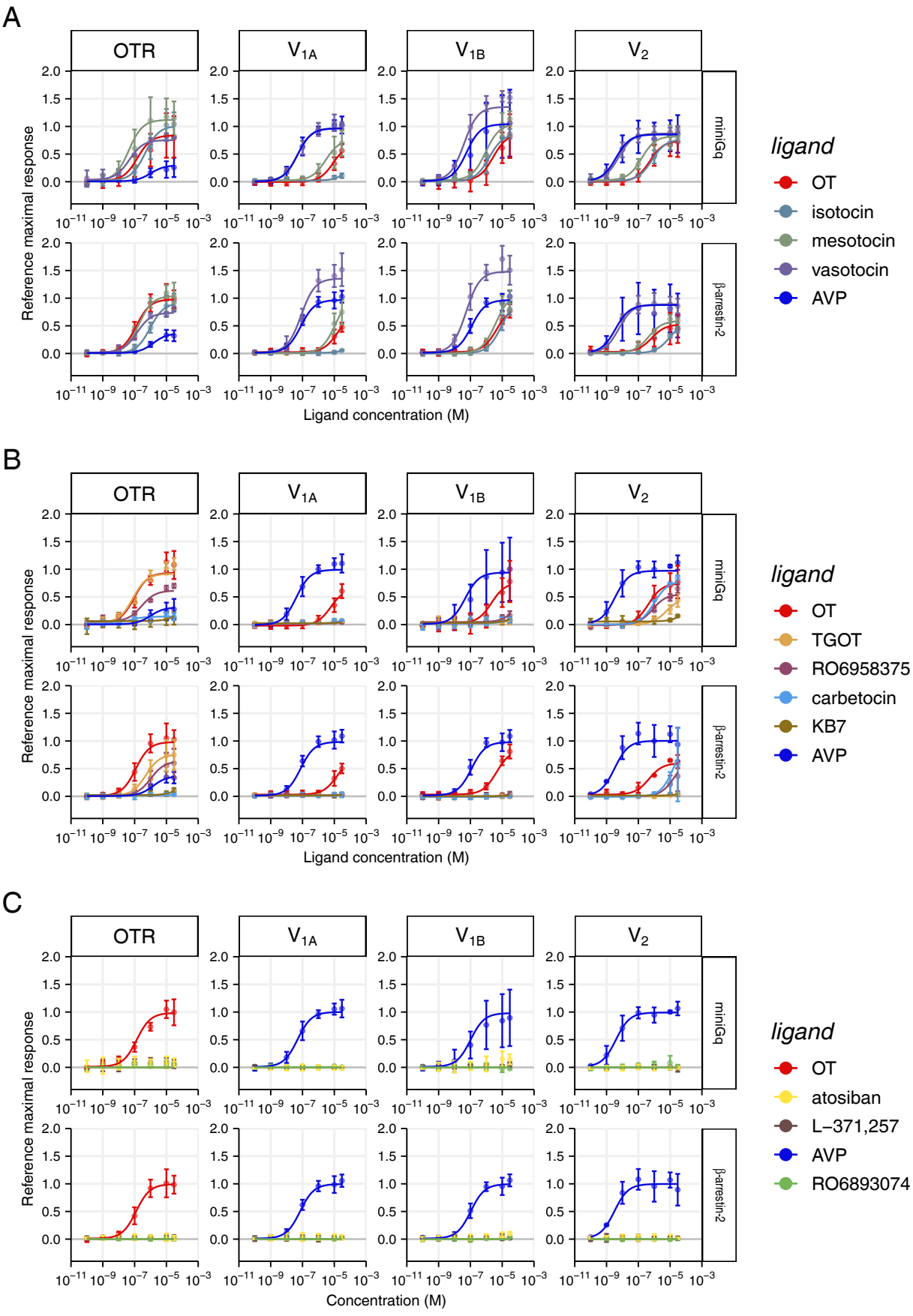

Figure S4: Relative efficacy and potency of orthologs and synthetic ligands on murine oxytocin and vasopressin receptors in Neuro-2a cells

(**A**) Relative dose-response of the synthetic ligands TGOT (mustard), RO6958375 (purple), carbetocin (light blue) and KB7 (light brown), as well as OT (red) and AVP (blue) on miniGq, and β-arrestin-2 recruitment profiles of mouse OTR, V_{1A}, V_{1B}, V_2 receptors in murine Neuro-2A cell lines. (**B**) Relative dose-response of the synthetic ligands TGOT (mustard), RO6958375 (purple), carbetocin (light blue) and KB7 (light brown) on miniGq, and β-arrestin-2 recruitments. (**C**) Relative dose-response of the antagonists atosiban (yellow), RO6893074 (green) and L-371,257 (dark brown) alone on miniGq, and β-arrestin-2 recruitments. The dose-response curve represents the mean of the biological replicates (n = 3-5 per sensor; Table S1).

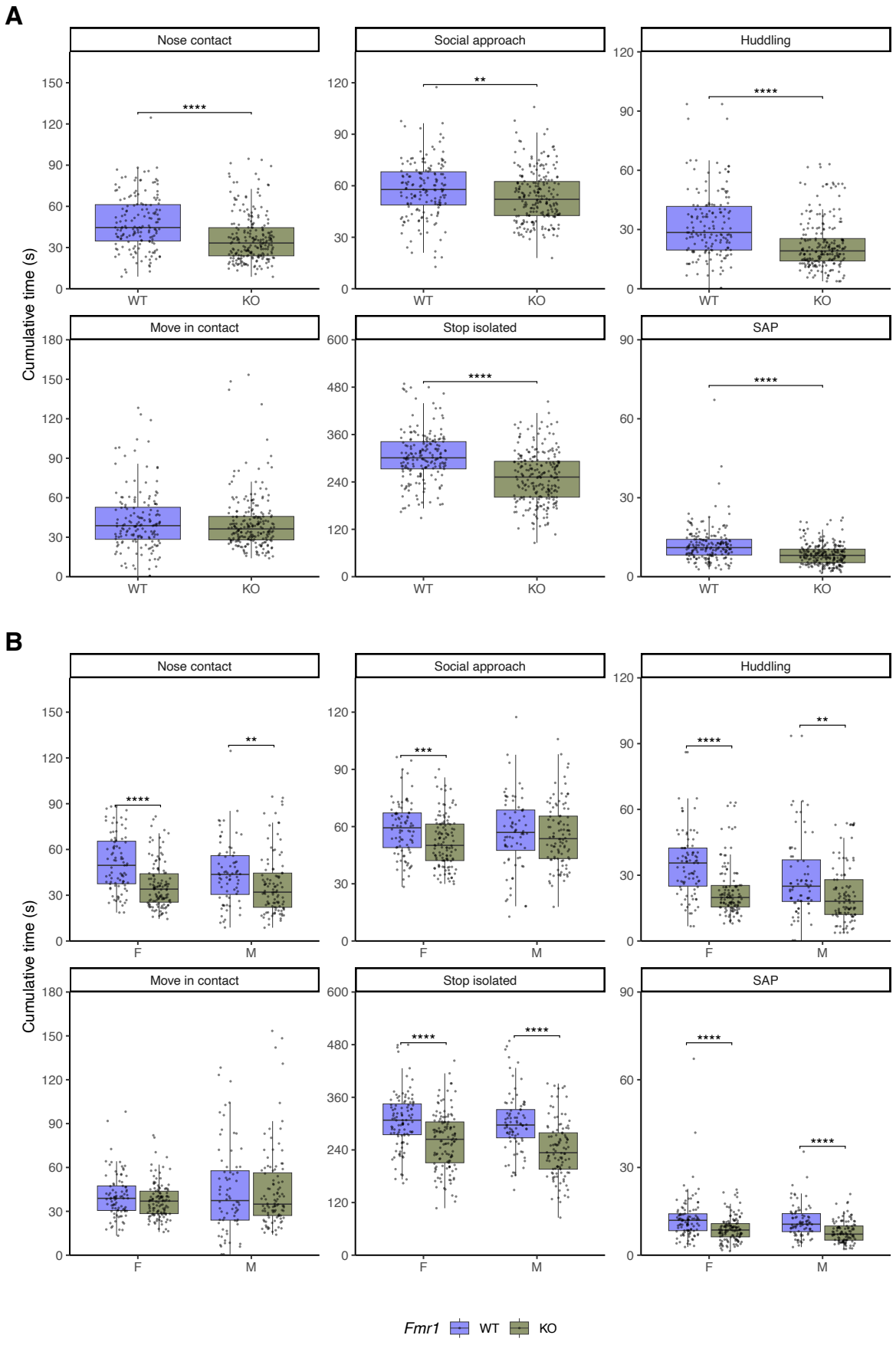

Figure S5: F*mr1* KO males and females display social impairments compared to WT mice in the Live Mouse Tracker

In the Live Mouse Tracker, the cumulative time in nose contact, social approach, huddling, 'move in contact', 'stop isolated' and SAP over a 10 min period were compared three days before the first administration between WT (purple; n = 188, 84 males and 104 females) and *Fmr1* KO (kaki; n = 235, 107 males and 128 females) mice (**A**) and between WT and *Fmr1* KO males and females (**B**). *Fmr1* KO mice showed reduced time spent in nose contact, social approach, huddling behaviour, isolation and stretch-attend posture compared to WT mice, independently of sex, with the exception of social approach in males. Data are presented as mean ± sd (raw values, mean and statistics in Table S2). Statistical analysis was conducted using Kruskal-Wallis tests followed by Dunn post hoc tests with asterisks indicating genotype or sex effect (p = P adjusted): *p<0.05, **p<0.01, ***p<0.001, ****p<0.0001. F, females; M, males; KO, *Fmr1* KO mice; SAP, Stretch-attend posture; WT, wild-type.

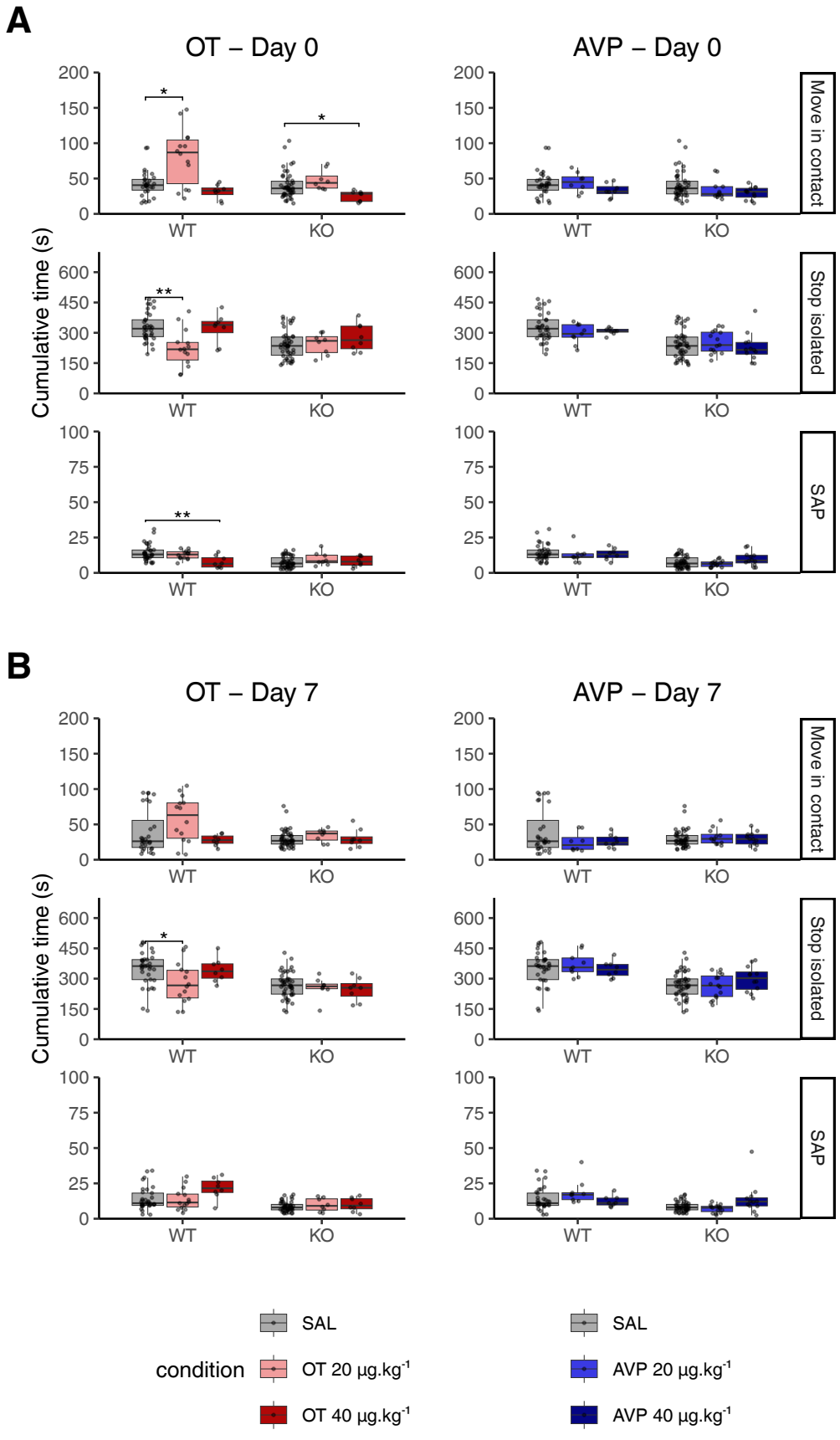

Figure S6: Effect of OT and AVP on social motivation, isolation and anxious-like behaviours in *Fmr1* KO and WT mice

In the Live Mouse Tracker, the cumulative time in 'move in contact', 'stop isolated' and SAP over a 10 min period were compared following 15 minutes of acute (**A**) or subchronic (**B**) intranasal administration of OT or AVP at low and moderate dose in WT (0 or NaCl 0.9% (grey): n = 34, 10 males and 24 females; OT 20 µg.kg^{-1} (pink): n = 14, 4 males and 10 females; OT 40 µg.kg^{-1} (red): n = 8, 4 males and 4 females; AVP 20 µg.kg^{-1} (light blue): n = 9, 5 males and 4 females; AVP 40 µg.kg^{-1} (dark blue): n = 8, 4 males and 4 females) and *Fmr1* KO mice (0 (grey): n = 46, 22 males and 24 females; OT 20 µg.kg^{-1} (pink): n = 8, 4 males and 4 females; OT 40 µg.kg^{-1} (red): n = 8, 4 males and 4 females; AVP 20 µg.kg^{-1} (light blue): n = 16, 5 males and 11 females; AVP 40 µg.kg^{-1} (dark blue): n = 12, 8 males and 4 females). Data are presented as mean ± sd (raw values, mean and statistics in Table S2). Statistical analysis was conducted using Kruskal-Wallis tests followed by Dunn post-hoc tests with asterisks indicating treatment effect (p = P adjusted): *p<0.05, **p<0.01, ***p<0.001, ****p<0.0001. AVP, vasopressin; OT, oxytocin; KO, *Fmr1* KO mice; SAL, saline; SAP, Stretch-attend posture; WT, wild-type.

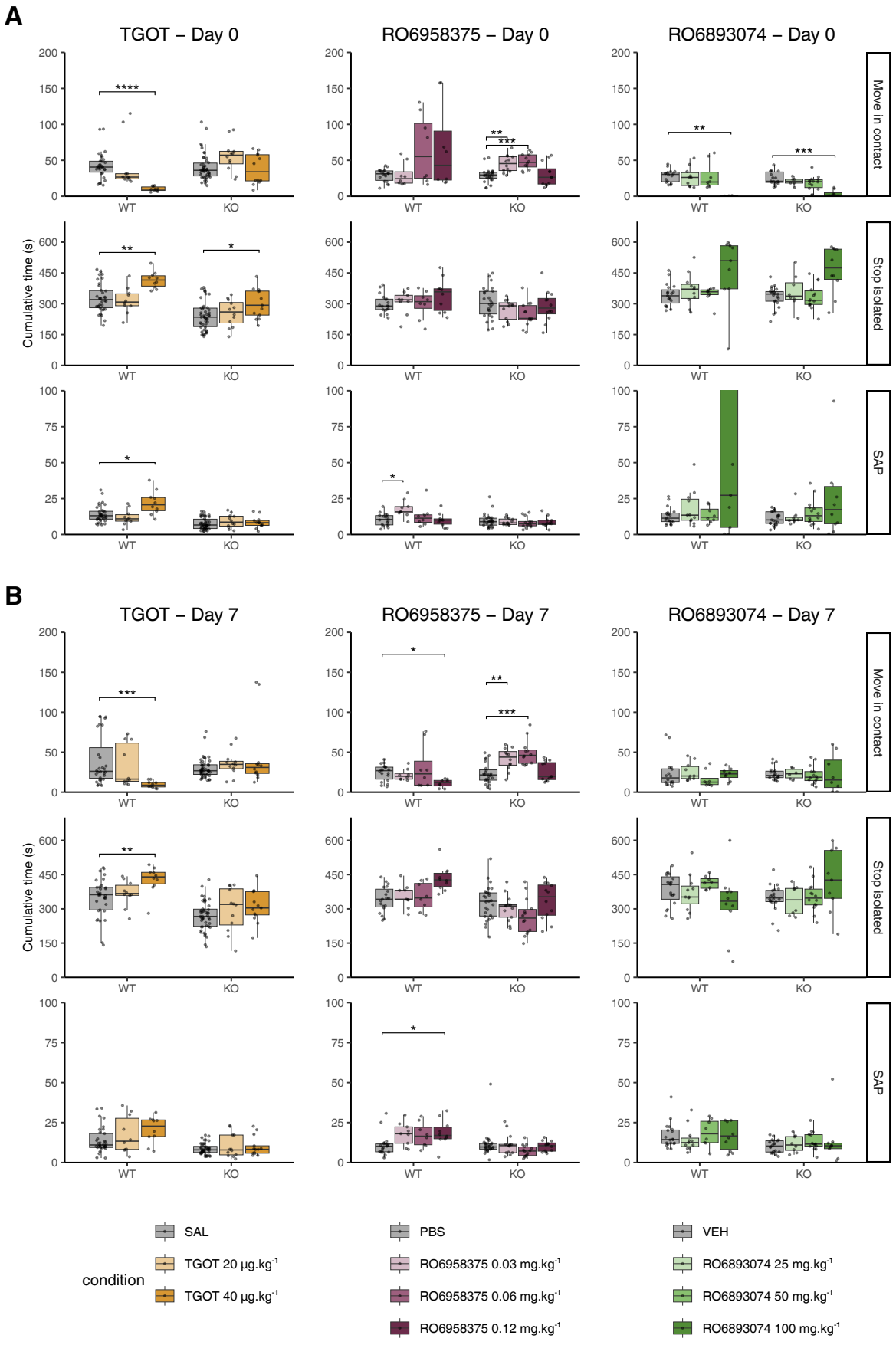

Figure S7: Effect of TGOT, RO6958375 and RO6893074 on social motivation, isolation and anxious-like behaviours in *Fmr1* KO and WT mice

In the Live Mouse Tracker, the cumulative time in 'move in contact', 'stop isolated' and SAP over a 10 min period were compared following 15 minutes of acute (**A**) or subchronic (**B**) administration of TGOT (intranasal) and RO6958375 (subcutaneous) OTR agonists and RO6893074 V_{1A} antagonist (intraperitoneal) at low, moderate and high dose in WT (0 = NaCl 0.9% for TGOT (grey): n = 34, 10 males and 24 females; TGOT 20 µg.kg^{-1} (light brown): n = 10, 4 males and 6 females; TGOT 40 µg.kg^{-1} (brown): n = 10, 6 males and 4 females; 0 = PBS 1X for RO6958375 (grey): n = 19, 10 males and 9 females; RO6958375 0.03 mg.kg^{-1} (light violet): n = 9, 5 males and 4 females; RO6958375 0.06 mg.kg^{-1} (violet): n = 8, 4 males and 4 females; RO6958375 0.12 mg.kg^{-1} (dark violet): n = 10, 5 males and 5 females; 0 = 0.1% Tween-80 for RO6893074 (grey): n = 20, 10 males and 10 females; RO6893074 25 mg.kg^{-1} (light green): n = 11, 5 males and 6 females;

RO6893074 50 mg.kg^{-1} (green): n = 8, 4 males and 4 females; RO6893074 100 mg.kg^{-1} (dark green): n = 10, 4 males and 6 females) and *Fmr1* KO mice (0 = NaCl 0.9% for TGOT (grey): n = 46, 22 males and 24 females; TGOT 20 µg.kg^{-1} (light brown): n = 12, 6 males and 6 females; TGOT 40 µg.kg^{-1} (brown): n = 13, 7 males and 6 females; 0 = PBS 1X for RO6958375 (grey): n = 27, 11 males and 16 females; RO6958375 0.03 mg.kg^{-1} (light violet): n = 13, 4 males and 9 females; RO6958375 0.06 mg.kg^{-1} (violet): n = 14, 5 males and 9 females; RO6958375 0.12 mg.kg^{-1} (dark violet): n = 12, 6 males and 6 females; 0 = 0.1% Tween-80 for RO6893074 (grey): n = 21, 11 males and 10 females; RO6893074 25 mg.kg^{-1} (light green): n = 9, 4 males and 5 females; RO6893074 50 mg.kg^{-1} (green): n = 14, 6 males and 8 females; RO6893074 100 mg.kg^{-1} (dark green): n = 10, 4 males and 6 females). Data are presented as mean ± sd (raw values, mean and statistics in Table S2). Statistical analysis was conducted using Kruskal-Wallis tests followed by Dunn post hoc tests with asterisks indicating treatment effect (p = P adjusted): *p<0.05, **p<0.01, ***p<0.001, ****p<0.0001. KO, *Fmr1* KO mice; OTR, oxytocin receptor; PBS, Phosphate-buffered saline; SAL, saline; SAP, stretch-attend postures; TGOT, (Thr⁸,Gly⁹)-oxytocin; VEH; vehicle; WT, wild-type.

SUPPLEMENTARY TABLES

Table S1: Pharmacological characteristics of ligands on murine oxytocin and vasopressin receptors in Neuro-2a cells

Receptor	Ligand	Emax		log(EC50)	
		Gq	barr2	Gq	barr2
OTR	AVP	0.93 ± 0.16 **	1.71 ± 0.35 ***	-6.06 ± 0.28 *	-5.88 ± 0.25 **
OTR	KB7	ND	ND	ND	ND
OTR	OT§	2.82 ± 0.38	4.84 ± 0.34	-6.75 ± 0.25	-6.89 ± 0.12
OTR	RO6958375	1.97 ± 0.26 *	3.15 ± 0.39 ***	-6.49 ± 0.27	-5.96 ± 0.15 ****
OTR	TGOT	3.08 ± 0.34	3.86 ± 0.37 **	-6.96 ± 0.25	-6.26 ± 0.14 ***
OTR	carbetocin	ND	ND	ND	ND
OTR	isotocin	3.47 ± 0.39	4.63 ± 0.37	-6.28 ± 0.19	-6.04 ± 0.10 ****
OTR	mesotocin	3.82 ± 0.35 *	5.30 ± 0.30	-7.34 ± 0.14 *	-6.72 ± 0.11
OTR	vasotocin	2.57 ± 0.33	3.73 ± 0.29 **	-7.18 ± 0.27	-6.86 ± 0.12
V1A	AVP§	5.99 ± 0.42	5.01 ± 0.37	-7.37 ± 0.09	-7.09 ± 0.13
V1A	KB7	ND	ND	ND	ND
V1A	OT	3.76 ± 0.50 ****	3.34 ± 0.83 *	-5.26 ± 0.13 ****	-4.87 ± 0.22 ****
V1A	RO6958375	0.26 ± 1.24 *	ND	-7.12 ± 1.65	ND
V1A	TGOT	ND	ND	ND	ND
V1A	carbetocin	ND	ND	ND	ND
V1A	isotocin	ND	ND	ND	ND
V1A	mesotocin	4.56 ± 0.56 *	5.54 ± 0.95	-5.61 ± 0.20 **	-4.91 ± 0.14 ****
V1A	vasotocin	6.02 ± 0.42	7.16 ± 0.42 ****	-7.33 ± 0.12	-7.09 ± 0.12
V1B	AVP§	2.92 ± 0.43	4.81 ± 0.44	-7.08 ± 0.23	-6.93 ± 0.10
V1B	KB7	ND	ND	ND	ND
V1B	OT	2.48 ± 0.71	4.09 ± 0.49	-5.44 ± 0.33 *	-5.36 ± 0.15 ****
V1B	RO6958375	ND	ND	ND	ND
V1B	TGOT	ND	ND	ND	ND
V1B	carbetocin	ND	ND	ND	ND
V1B	isotocin	2.38 ± 0.61	4.94 ± 0.76	-5.78 ± 0.30 *	-5.06 ± 0.15 ****
V1B	mesotocin	3.05 ± 0.54	5.42 ± 0.50	-5.86 ± 0.24 *	-5.43 ± 0.11 ****
V1B	vasotocin	3.92 ± 0.48	7.46 ± 0.37 ***	-7.27 ± 0.19	-7.26 ± 0.07 **
V2	AVP§	3.53 ± 0.24	5.59 ± 0.43	-8.33 ± 0.18	-8.43 ± 0.12
V2	KB7	ND	ND	ND	ND
V2	OT	3.04 ± 0.29	3.39 ± 0.35 **	-6.27 ± 0.15 ***	-6.20 ± 0.18 ***
V2	RO6958375	2.29 ± 0.37	4.06 ± 0.85 *	-5.97 ± 0.32 *	-4.80 ± 0.20 ****
V2	TGOT	1.83 ± 1.01	ND	-5.27 ± 0.37 *	ND
V2	carbetocin	3.24 ± 0.46	7.05 ± 0.93 *	-5.98 ± 0.17 **	-4.75 ± 0.15 ****
V2	isotocin	3.21 ± 0.39	3.49 ± 0.96 **	-6.14 ± 0.17 ***	-5.14 ± 0.22 ****
V2	mesotocin	3.50 ± 0.31	3.98 ± 0.32 **	-6.74 ± 0.18 ***	-6.35 ± 0.11 ****
V2	vasotocin	3.69 ± 0.29	5.87 ± 0.31	-8.16 ± 0.14	-8.20 ± 0.08

Table S2: Pharmacological characteristics of OT and AVP on human oxytocin and vasopressin receptors in HEK293A cells

Receptor	Ligand	Emax		log(EC50)	
		Gq	barr2	Gq	barr2
OTR	AVP	ND	0.44 ± 0.17 ***	ND	-6.47 ± 0.74
OTR	OT§	0.83 ± 0.16	1.44 ± 0.18	-6.69 ± 0.48	-7.12 ± 0.30
V_{1A}	AVP§	5.29 ± 0.42	3.32 ± 0.25	-8.12 ± 0.14	-7.93 ± 0.13
V_{1A}	OT	1.01 ± 0.17 ***	0.43 ± 0.10 ****	-7.18 ± 0.42 *	-7.30 ± 0.69
V_{1B}	AVP§	3.25 ± 0.28	3.01 ± 0.20	-8.19 ± 0.25	-8.55 ± 0.19
V_{1B}	OT	2.13 ± 0.35 *	1.60 ± 0.30 ****	-6.19 ± 0.24 ***	-5.84 ± 0.28 ****
V2	AVP§	5.46 ± 0.42	8.71 ± 0.48	-8.06 ± 0.13	-8.20 ± 0.10
V2	OT	3.93 ± 0.45 *	4.27 ± 0.43 ****	-6.49 ± 0.16 ***	-6.23 ± 0.13 ****

Table S3: List of parameters for each model equation and model selection

The table reports the parameter search intervals (in log10 scale) for the first model (equation **(4)** in the material and method), the maximum likelihood estimate and their profile-based confidence intervals for the first model (equation **(4)** in the material and method), the parameter search intervals (in log10 scale) for the second model (equation **(6)** in the material and method), the maximum likelihood estimate and their profile-based confidence intervals for the second model (equation **(6)** in the material and method), and the model selection calculations.

Parameters_model_1

Parameter Name	parameterScale	lowerBound	upperBound
k_rec	log10	0.000001	100
k_tau	log10	0.0001	100
k_int	log10	0.001	10
KD	log10	1,00E-12	0.1
kbret,1	log10	0.001	1000
kbret,2	log10	0.001	1000
kbret,3	log10	0.001	1000
sd_1	log10	0.001	10
sd_2	log10	0.001	10
sd_3	log10	0.001	10

MLE_CI_model_1

		OTR		V1A		V1B		V2	
Normalised parameter name	**parameter value**	**OT**	**AVP**	**OT**	**AVP**	**OT**	**AVP**	**OT**	**AVP**
k_rec	MLE	-0,98	-6,00	0,29	-0,64	-1,31	-1,08	-1,27	-0,24
	left CI	-1,04	-6,00	0,08	-0,70	-1,37	-1,13	-1,41	-0,31
	right CI	-0,91	0,08	0,57	-0,57	-1,25	-1,03	-1,16	-0,18
k_tau	MLE	-1,38	2,00	2,00	-0,65	-0,75	-0,73	-0,66	0,32
	left CI	-1,47	1,63	1,03	-0,74	-0,82	-0,79	-0,77	0,11
	right CI	-1,29	2,00	2,00	-0,55	-0,69	-0,67	-0,55	0,49
k_int	MLE	-0,21	-2,30	-1,14	-0,65	-0,21	-0,33	-0,56	-1,32
	left CI	-0,24	-2,38	-1,23	-0,70	-0,25	-0,37	-0,63	-1,42
	right CI	-0,17	-2,06	-1,06	-0,61	-0,18	-0,30	-0,49	-1,19
KD	MLE	-6,44	-4,43	-2,41	-6,36	-5,04	-6,69	-5,63	-8,09
	left CI	-6,46	-4,58	-3,32	-6,40	-5,07	-6,71	-5,68	-8,16
	right CI	-6,41	-4,33	-2,26	-6,33	-5,01	-6,66	-5,58	-8,02
sd_1	MLE	-1,62	-1,69	-1,71	-1,65	-1,71	-1,62	-1,73	-1,68
	left CI	-1,64	-1,71	-1,72	-1,67	-1,73	-1,63	-1,74	-1,69
	right CI	-1,61	-1,68	-1,69	-1,64	-1,70	-1,60	-1,71	-1,66
sd_2	MLE	-1,70	-1,82	-1,89	-1,60	-1,75	-1,61	-1,78	-1,66
	left CI	-1,71	-1,83	-1,91	-1,61	-1,76	-1,62	-1,79	-1,67
	right CI	-1,69	-1,81	-1,88	-1,59	-1,73	-1,60	-1,77	-1,64
sd_3	MLE	-1,52	-1,69	-1,62	-1,47	-1,55	-1,47	-1,71	-1,70
	left CI	-1,53	-1,70	-1,63	-1,48	-1,56	-1,48	-1,72	-1,71
	right CI	-1,51	-1,68	-1,61	-1,47	-1,54	-1,46	-1,70	-1,69
kbret_1	MLE	-0,42	-1,36	-0,89	-0,62	-0,72	-0,71	-0,79	-0,85
	left CI	-0,46	-1,38	-0,95	-0,66	-0,73	-0,72	-0,82	-0,88
	right CI	-0,37	-1,34	-0,82	-0,58	-0,70	-0,69	-0,76	-0,80
kbret_2	MLE	0,83	-1,03	-0,72	0,22	0,46	0,41	-0,27	-0,50
	left CI	0,75	-1,04	-0,81	0,15	0,41	0,37	-0,35	-0,56
	right CI	0,90	-1,00	-0,63	0,29	0,51	0,46	-0,19	-0,41
kbret_3	MLE	-0,63	-0,60	-1,16	-0,80	-0,89	-0,81	-1,26	-0,89
	left CI	-0,67	-0,81	-1,29	-0,83	-0,91	-0,82	-1,29	-0,91
	right CI	-0,59	-0,51	-0,98	-0,77	-0,88	-0,79	-1,23	-0,86

Parameters_model_2

Parameter Name	parameterScale	lowerBound	upperBound
k_tau	log10	0.0001	100
k_int	log10	0.001	10
KD	log10	1,00E-12	0.1
sd_1	log10	0.001	10
sd_2	log10	0.001	10
sd_3	log10	0.001	10
kbret_1	log10	0.001	1000
kbret_2	log10	0.001	1000
kbret_3	log10	0.001	1000

MLE_CI_model_2

		OTR		V1A		V1B		V2	
Normalised parameter name	parameter value	OT	AVP	OT	AVP	OT	AVP	OT	AVP
k_tau	MLE	-1,96	2,00	2,00	1,01	-1,26	-1,32	-0,59	0,78
	left CI	-2,03	1,63	1,56	0,92	-1,30	-1,36	-0,72	0,70
	right CI	-1,90	2,00	2,00	1,09	-1,21	-1,29	-0,45	0,87
k_int	MLE	-0,11	-2,30	-1,40	-1,59	-0,03	-0,13	-0,64	-1,63
	left CI	-0,14	-2,38	-1,50	-1,64	-0,06	-0,16	-0,72	-1,69
	right CI	-0,08	-2,06	-1,30	-1,55	0,00	-0,10	-0,56	-1,58
KD	MLE	-6,47	-4,43	-2,64	-5,81	-5,16	-6,84	-5,62	-7,95
	left CI	-6,49	-4,58	-3,05	-5,86	-5,19	-6,86	-5,67	-7,99
	right CI	-6,45	-4,33	-2,47	-5,76	-5,13	-6,81	-5,57	-7,91
sd_1	MLE	-1,56	-1,69	-1,70	-1,64	-1,64	-1,52	-1,72	-1,67
	left CI	-1,58	-1,71	-1,72	-1,65	-1,65	-1,54	-1,74	-1,68
	right CI	-1,55	-1,68	-1,69	-1,62	-1,63	-1,51	-1,71	-1,65
sd_2	MLE	-1,70	-1,82	-1,89	-1,56	-1,75	-1,59	-1,77	-1,66
	left CI	-1,71	-1,83	-1,90	-1,58	-1,76	-1,60	-1,79	-1,67
	right CI	-1,68	-1,81	-1,87	-1,55	-1,73	-1,57	-1,76	-1,64
sd_3	MLE	-1,53	-1,69	-1,62	-1,48	-1,56	-1,48	-1,71	-1,70
	left CI	-1,54	-1,70	-1,63	-1,49	-1,57	-1,49	-1,72	-1,71
	right CI	-1,52	-1,68	-1,61	-1,47	-1,55	-1,48	-1,70	-1,69
kbret_1	MLE	-0,26	-1,36	-1,02	-0,96	-0,67	-0,63	-0,84	-0,91
	left CI	-0,30	-1,38	-1,06	-0,97	-0,68	-0,64	-0,86	-0,92
	right CI	-0,22	-1,34	-0,97	-0,95	-0,66	-0,62	-0,81	-0,90
kbret_2	MLE	1,36	-1,03	-0,78	-0,50	0,85	0,88	-0,32	-0,64
	left CI	1,30	-1,04	-0,86	-0,52	0,81	0,85	-0,42	-0,66
	right CI	1,42	-1,00	-0,70	-0,48	0,89	0,91	-0,23	-0,61
kbret_3	MLE	-0,49	-0,60	-1,40	-0,81	-0,85	-0,75	-1,30	-0,84
	left CI	-0,53	-0,81	-1,49	-0,84	-0,86	-0,76	-1,33	-0,87
	right CI	-0,44	-0,51	-1,32	-0,78	-0,84	-0,73	-1,28	-0,81

Model_selection

receptor	ligand	best_obj	ndata	model	npar	lrt_stat	lrt_pvalue	aic	bic
OTR	OT	-19 552,44	8820	model_2	9	523,28	8,20E-116	525,28	532,36
		-19 814,07	8820	model_1	10	0	1	0	0
V1A		-22 145,73	8820	model_2	9	69,26	8,64E-17	71,26	78,34
		-22 180,36	8820	model_1	10	0	1	0	0
V1B		-20 557,43	8820	model_2	9	542,40	5,66E-120	544,40	551,49
		-20 828,63	8820	model_1	10	0	1	0	0
V2		-22 512,59	8785	model_2	9	59,57	1,18E-14	61,57	68,65
		-22 542,37	8785	model_1	10	0	1	0	0
OTR	AVP	-22 426,93	8785	model_2	9	0	1	0	0
		-22 426,93	8785	model_1	10	1,29E-05	NA	-2,00	-9,08
V1A		-18 724,91	8820	model_2	9	529,27	4,07E-117	531,27	538,35
		-18 989,54	8820	model_1	10	0	1	0	0
V1B		-18 358,01	8820	model_2	9	885,58	1,34E-194	887,58	894,67
		-18 800,81	8820	model_1	10	0	1	0	0
V2		-21 611,89	8820	model_2	9	69,91	6,19E-17	71,91	79,00
		-21 646,85	8820	model_1	10	0	1	0	0

Table S4: Results for RO6893074 from the CEREP selectivity screen. The table reports the percentage of inhibition at 3 µM of the RO6893074 on 35 human receptors, channels or transporters, as well 12 human enzymes tested in functional assays and reported as percentage enzyme inhibition over basal activity. Enzyme assays are noted with an asterisk*. Negative numbers are due to assay noise.

Assay	% inhibition at 3µM	Assay	% inhibition at 3µM
A1 (h) (agonist radioligand)	-1	5-HT2B (h) (agonist radioligand)	51
A3 (h) (agonist radioligand)	-10	5-HT3 (h) (antagonist radioligand)	5
alpha 1A (h) (antagonist radioligand)	5	sigma (non-selective) (h) (agonist radioligand)	-2
alpha 2A (h) (antagonist radioligand)	6	sst4 (h) (agonist radioligand)	32
beta 1 (h) (agonist radioligand)	-2	GR (h) (agonist radioligand)	-9
AT1 (h) (antagonist radioligand)	-1	ERalpha (h) (agonist fluoligand)	2
BZD (central) (agonist radioligand)	2	AR (h) (agonist radioligand)	-17
D1 (h) (antagonist radioligand)	-12	Ca2+ channel (L, diltiazem site) (benzothiazepines) (antagonist radioligand)	5
D2S (h) (agonist radioligand)	2	Na+ channel (site 2) (antagonist radioligand)	1
glycine (strychnine-insensitive) (antagonist radioligand)	-2	norepinephrine transporter (h) (antagonist radioligand)	5
H1 (h) (antagonist radioligand)	0	5-HT transporter (h) (antagonist radioligand)	-11
H2 (h) (antagonist radioligand)	-11	*COX2 (h)	9
H3 (h) (agonist radioligand)	-13	*PDE5 (h) (non-selective)	-15
MT3 (ML2) (agonist radioligand)	45	*ACE (h)	-22
M2 (h) (antagonist radioligand)	2	*HIV-1 protease (h)	2
M4 (h) (antagonist radioligand)	10	*CDK2 (h) (cycA)	-3
N muscle-type (h) (antagonist radioligand)	-3	*GSK3alpha (h)	-1
kappa (KOP) (agonist radioligand)	29	*GSK3beta (h)	-1
mu (MOP) (h) (agonist radioligand)	6	*ZAP70 kinase (h)	-17
PPARgamma (h) (agonist radioligand)	14	*acetylcholinesterase (h)	7
FP (h) (agonist radioligand)	10	*MAO-A (h)	11
5-HT1A (h) (agonist radioligand)	-12	*MAO-B (h) recombinant enzyme	0
5-HT2A (h) (agonist radioligand)	-4	*xanthine oxidase/ superoxide O2- scavenging	-6

Table S5: raw, mean, standard deviation and statistics of social interaction in the Live Mouse Tracker